Journal of Chromatography, 500 (1990) 95–138
Elsevier Science Publishers B.V., Amsterdam — Printed in The Netherlands

CHROM. 22 027

HYPERCOULOMETRY OF THE SECOND KIND IN ELECTRON-CAPTURE DETECTION[a]

WALTER A. AUE*
Department of Chemistry, Dalhousie University, Halifax, Nova Scotia B3H 4J3 (Canada)
and
K. W. MICHAEL SIU, DIANE BEAUCHEMIN[b] and SHIER S. BERMAN
Division of Chemistry, National Research Council, Montreal Road, Ottawa, Ontario (Canada)
(First received June 7th, 1989; revised manuscript received September 20th, 1989)

SUMMARY

Hypercoulometry in electron-capture detectors (ECDs) has been repeatedly described in the literature, and has been attributed to the space charge effect of analyte-derived anions migrating to the anode beyond the radioactive plasma [W. A. Aue and S. Kapila, *J. Chromatogr.*, 188 (1980) 1]. However, the existence of a *different* kind of hypercoulometry has recently been suggested by experiments using clean pulse conditions in a small-volume electron-capture detector [K. W. M. Siu, G. J. Gardner and S. S. Berman, *J. Chromatogr.*, 330 (1985) 87].

The present study provides a speculative explanation of this "second kind" of hypercoulometry by relying on computer-aided simulation, and by using apparent rate constants from a measurement of ECD steady states under unipolar and bipolar drive conditions [K. W. M. Siu, S. S. Berman and W. A. Aue, *J. Chromatogr.*, 408 (1987) 53].

Two salient features of this hypercoulometric response (vis-a-vis conventional ECD mechanisms) are that the rate constant for anion–cation neutralization is significantly smaller than the one for electron–cation recombination and that overall electrical neutrality prevails. As one of the consequences, steady state takes a much longer time to reach than in conventional model systems.

The simulation characterizes "hypercoulometry of the second kind" as the charge effect of non-collected, analyte-derived anions in or near the radioactive plasma, which causes a larger cation concentration and hence a higher electron–cation recombination rate. Given certain simplifying assumptions, the effect can be approximated to a large extent by conventional, *i.e.* "stirred reactor" type kinetic modelling. The model is capable of producing strongly hypercoulometric response profiles that agree well with the experimental profiles measured earlier in the same detector [K. W. M. Siu, G. J. Gardner and S. S. Berman, *J. Chromatogr.*, 330 (1985) 87].

---

[a] Presented in part at the *70th CIC Conference, Quebec City, June 1987*. NRCC 31028.
[b] Present address: Department of Chemistry, Queen's University, Kingston, Ontario, Canada.

0021-9673/90/$03.50

Even when hypercoulometry is not observed, the internal detector processes remain the same. It is therefore suggested that a large proportion of hypocoulometric response in well-performing detectors also results from a protracted presence of anions and, in turn, an increase in the electron–cation recombination rate.

INTRODUCTION

Hypercoulometry

Hypercoulometry is the disturbing but, more importantly, interesting and useful condition in which an electron-capture detector appears to consume more electrons than it is being fed molecules of analyte, *i.e.* e/m or F/mol > 1. The ratio of "electrons apparently captured" to "molecules introduced", or of "faradays peak area" to "moles analyte injected", has been called the coulometric or, if it routinely exceeds unity, the hypercoulometric ratio.

Hypercoulometry is disturbing because it injects an element of uncertainty into the electron-capture detector's use as a "gas-phase coulometer"[1–5], *i.e.* it questions the existence of an "absolute" mode that does not need standards or calibration curves (but does require that F/mol be equal to unity). Further, hypercoulometry is interesting because the precise mechanism(s) that cause it are not immediately obvious. And, finally, hypercoulometry is useful because it provides a detector with superior sensitivity.

The most pronounced hypercoulometric effects have been found in a pressurized d.c.-electron-capture detector (ECD), reaching F/mol values of about 50 at 5 atm and still increasing with pressure[6]. However, it is also quite possible to obtain hypercoulometric performance at ambient pressure and under a wide range of pulse conditions for both associative and dissociative electron capturers. For instance, carbon tetrachloride reaches a value of 8 F/mol with a pulse width of 0.5 μs, a pulse interval of 100 μs and a pulse amplitude of 20 or 40 V, *i.e.* at what have been called "field-free" conditions[7].

Hypercoulometry in a large, asymmetric, d.c.-driven detector arises from space-charge phenomena that, in essence, amplify the initial electron-capture reaction. To recapitulate shortly, electrons can captured *outside* the radioactive plasma, leading to a space charge of anions that travel slowly toward the anode and cannot be neutralized by the remote cations. The negative space charge steepens the potential gradient over the unipolar and flattens it over the bipolar region. A flatter potential gradient over the bipolar plasma region means longer residence times for cations and electrons, hence a higher rate of recombination. It is easy to demonstrate that a single anion can thus lead to the recombination of several cation–electron pairs[8]. Recently, an *ab initio* calculation of spatially and temporally resolved ECD reactions and ion movements proved the validity of the concept[9]. This applies not only to the common d.c. and pulse regimes, but also to a.c. polarization[10].

That mechanism for producing hypercoulometry is favored by a short-range radioactive isotope, a long interelectrode distance, and elevated pressure; all conditions that promote heterogeneity of charge distribution in the detector cell. It was therefore a bit surprising to find very clear evidence of hypercoulometry occurring in a small-volume detector with a Ni-63 foil[7] —and we have wondered ever since whether

there do exist hypercoulometric mechanisms of kinds other than the one we described some time ago[8].

There also existed a number of possibly related questions that had come up over the years and that could not yet be answered to our satisfaction. For instance: What is the residence time of analyte-derived anions in an ECD under typical pulse conditions? How do anion concentrations tie in with cation concentrations and residence times?

A recent study of ours[11] determined apparent recombination (cation–electron) and neutralization (cation–anion) rate constants from experiments carried out with the *same* small-volume detector that, earlier on, had provided such clear evidence of hypercoulometry[7]. This gives us now the chance to simulate hypercoulometry based on kinetic data valid for this very detector.

Detector asymmetry, plasma heterogeneity and electrical anisotropy

It should be noted that such a simulation can, at best, *approximate* the real system. Well functioning electron-capture detector have in general strongly heterogeneous plasma distributions[8,12,13], and most types of simulations must take this into account. It is possible to simulate, in a rigorous way, spatially resolved charge transport and kinetics but, so far, this has been done only for a parallel-plate system[9,10]. The detector used in the newer experiments[11], however, has a relatively long, cylindrical cathode of small radius, and an axially offset anode; conditions that would make it extremely difficult to model the initial ion pair distribution and the combination of externally imposed and internally generated electrical fields. We decided, therefore, to combine certain charge postulates with a numerical approach that considers temporal but disregards spatial heterogeneity. Disregarding spatial heterogeneity cannot be justified in a strictly quantitative sense, but it seems acceptable for the approximate kinetic description of an extremely slender, rod-like detector cell. Also, as will be seen later, it produces results that agree well with experimental data.

Yet, since all of this work thus uses the kinetic formalism that is appropriate to a homogeneous mixture (the "stirred reactor" concept), we hasten to add that the Varian detector upon which this study is modelled and which provided the apparent rate constants and experimental response profiles, *cannot* be considered homogeneous under typical ECD drive conditions. This has been clearly established by experiment. Perhaps a few comments on plasma homogeneity, electrical isotropy and detector symmetry are in order.

A perfectly symmetrical detector, based on the presence of a homogeneous plasma and the absence of space-charge effects (for instance an idealized parallel-plate system), must by definition be electrically isotropic, *i.e.* it must exhibit the same impedance toward the passage of current in one or the other of the two possible electrical field directions. For instance, the I/V profile of such a system operated in d.c. mode should be the same whether the radioactive foil serves as the cathode ("regular field") or the anode ("reversed field"). Also, it should give the same response to analyte whether operated in regular- or reversed-field direction.

Obviously, such a system does not exist (and if it did, would likely be incapable of good analytical performance). More importantly, the particular geometry of the Varian detector —its very small volume, its very pronounced electrical asymmetry— suggest that a conceptual distinction be made between plasma homogeneity and electrical isotropy. The ECD is not a purely electrical system and its impedance is, if

one wishes to define it that way, as well a *chemical* one[8]. How much current is passed under a particular electrical field depends on a complex, both spatially and temporally varying interplay of (a) the ion pair generation rate (and, if analyte is present, the analyte electron-capture rate); (b) the cation–electron recombination rate (and, with analyte, the cation–anion neutralization rate); (c) the speed of migration, respectively residence time, of charged particles; and (d) the space charges that control current flow, even on a short-time scale. As a rule of thumb, it is the migration of *cations* (plus, in the presence of analyte, anions) that determine the size at the current[8]. This is the (major) reason why the radioactive foil in a well-functioning detector is always the cathode: the cations must take the shorter, the electrons (and anions) the longer path; and the faster it is for the cations and the slower it is for the electrons to travel, *i.e.* the greater a difference the appearance of anions is going to make, the larger is the response. The Varian detector represents, in this regard, an extreme case of electrical anisotropy achieved primarily by asymmetric electrode geometry rather than, as for instance in the case of a parallel-plate design, primarily by asymmetric ion pair generation. This, then, is the reason why we feel justified, reaction-wise, to approximate the modus operandi of this detector by a stirred-reactor formalism, despite the detector's very large electrical anisotropy. This anisotropy is quantitatively illustrated by the d.c. response and current profiles shown in Fig. 1. As other well-performing ECD systems, this detector will provide adequate response only in one of the two possible directions in which an electrical field can be imposed, regardless of which drive mode (d.c. pulse, etc.) is used.

This electrical anisotropy was also one of the reasons why we designated the rate constants determined by using this detector as "apparent"[11]. Yet, to simulate

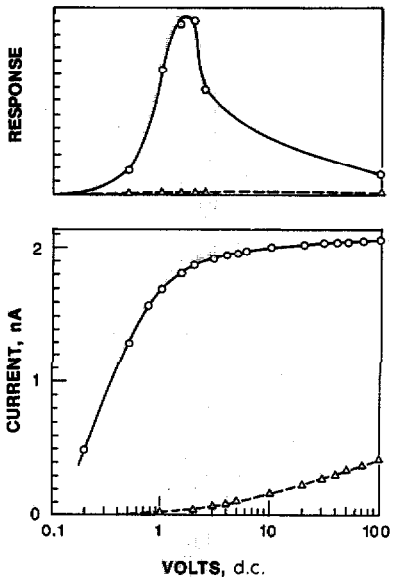

Fig. 1. Response and current profiles in a Varian electron-capture detector under a d.c. regime. Analyte: 10 pg lindane. Carrier gas (nitrogen) flow (external): 25 ml/min. Detector temperature: 220°C. Full line: regular field direction; dashed line: reversed-field direction.

processes in, and compare them to actual responses from, this detector, the "apparent" constants should serve better than the "true" physicochemical ones (even if the latter were available). The chain of calculation is thus clearly circular, but that may actually help in establishing whether ECD response can be successfully modelled by entering only experimental conditions —*i.e.* input and reaction rate constants but no fudge factors— even though these constants pertain to only one particular system. In other words, some of the errors committed in considering the system to be homogeneous from a kinetic methodology point of view, would be similarly represented in the determination of apparent constants[11] and in the simulation of response, and would therefore tend to cancel each other.

Simplest kinetic models

Accepting this premise and thereby accepting particle homogeneity as an expedient starting position, we can use the conventional basic equations[14,15] for creation, transfer and destruction (but not yet collection) of charge, *viz.*:

the initial creation of ion pairs by β radiation,

$$M + \beta \xrightarrow{S_{IP}} M^+ + e^- + \beta \text{ (lower energy)} \tag{1}$$

the recombination of these ion pairs,

$$M^+ + e^- \xrightarrow{k_R} M \tag{2}$$

the capture of electrons by analyte molecules,

$$A + e^- \xrightarrow{k_C} A^- \tag{3}$$

and the neutralization of analyte-derived anions;

$$A^- + M^+ \xrightarrow{k_N} \text{neutral products} \tag{4}$$

together with the thereby defined rate equations for electrons,

$$\frac{d[e^-]}{dt} = S_{IP} - k_C[A][e^-] - k_R[M^+][e^-] \tag{5}$$

cations,

$$\frac{d[M^+]}{dt} = S_{IP} - k_R[M^+][e^-] - k_N[M^+][A^-] \tag{6}$$

anions,

$$\frac{d[A^-]}{dt} = k_C[A][e^-] - k_N[A^-][M^+] \tag{7}$$

and analyte,

$$\frac{d[A]}{dt} = S_A - k_C[A][e^-] \tag{8}$$

wherein S_{IP} is the (constant) supply rate of ion pairs and S_A is the (constant or Gaussian) supply rate of analyte, both in particles per cm^3 per s; k_R, k_N and k_C are the rate constants for recombination, neutralization and capture in cm^3/s; e^- designates the electron, and M^+ and A^- stand for any cation and analyte-derived anion, respectively (the exact nature of these species depending on carrier gas contamination, chemical structure of the analyte, the extent of clustering reactions, etc.); and concentration terms, [ ], are given in particles per cm^3. The simulation will involve iterative solutions of the simultaneous rate equations, and will be carried out for a large number of different cases. To distinguish between baseline ($S_A = 0$) and peak ($S_A > 0$) conditions, the former will usually be referred to as the "clean", the latter as the "doped" system.

While that approach is the most rigorous, it is not the simplest and quite possibly not even the most accurate. All rates and rate constants have been measured in the very system the iterative procedure tries to simulate, with the exception of the electron capture constant k_C. Values for the "true" constant of the model analyte SF_6 are available from the literature, and one of these values is, in fact, being used for parts of this study. However, in the real detector there must be differences in analyte concentration along the flowpath through the long, slender foil cylinder, and there must be radial differences in local electron concentrations as well; rendering questionable the use of a constant whose definition is predicated on the homogeneity of the system it attempts to describe.

Fortunately, a variety of experiments in the literature have shown that it is quite possible to convert almost all analyte molecules to anions, provided the analyte has a high capture cross-section, is introduced only in small amounts, and remains present in the system for a comparatively long time. If we choose such conditions and disregard the time delay involved in forming the anions (an approach that is quite reasonable on, say, a one-second timescale) then the analyte introduction rate can be equated with the anion generation rate,

$$S_A = S_{A^-} \tag{9}$$

in what amounts, simulation-wise, to an instantaneous conversion of analyte molecules to anions (*i.e.* algorithmic coulometry on the molecular level). The use of eqn. 9 is obviously limited by the conditions outlined above, and it has been used in this sense in our earlier derivation[11] of k_N and k_R as well. However, in order to establish that it is essentially correct, *i.e.* that its aberrations in time and concentration remain tolerable, a comparison of simulations using eqns. 5–8 on one hand, and the same equations simplified according to eqn. 9 on the other, will be carried out for a few typical cases.

The limited use of eqn. 9 reduces the working equations to

$$\frac{d[e^-]}{dt} = S_{IP} - S_A - k_R[M^+][e^-] \tag{10}$$

$$\frac{d[A^-]}{dt} = S_A - k_N[M^+][A^-] \tag{11}$$

$$\frac{d[M^+]}{dt} = S_{IP} - k_R[M^+][e^-] - k_N[M^+][A^-] \tag{12}$$

for incremental (stepwise) solution through time. In fact, this simplifies the computation to the point that the first, exploratory simulations of this study could be carried out with the assistance of only a very simple pocket calculator.

In our case, the analyte is given relevant properties of SF_6, since this compound happens to be one of the strongest and, in practical and theoretical terms, best characterized electron capturers. The capture constant $k_C = 3 \cdot 10^{-7}$ cm^3/s represents the SF_6 literature value[16]. The recombination constant $k_R = 2.9 \cdot 10^{-5}$ and the neutralization constant $k_N = 3.8 \cdot 10^{-7}$ cm^3/s are results of measurements on SF_6 in N_2, which used the small-volume Varian detector and are subject to certain limitations[11]. The detector itself has been well described[17]. Its ion pair generation rate S_{IP} is about $2.0 \cdot 10^{-9}$ A or $3.5 \cdot 10^{10}$ particles per cm^3 per s. Using these data, we shall start with a simple thought experiment.

Although imaginary as far as a real-life ECD is concerned, one can fairly easily simulate the approach to steady state that would occur if (a) the system behaved in a homogeneous manner; (b) it started from zero for all particle concentrations; (c) no electrical field would be imposed; (d) analyte introduction, as a first approximation, occurred slow on the timeframe of the equations above; and (e) no selective ventilation, diffusion, etc. effects were present. Under these conditions, charge neutrality must prevail exactly,

$$[M^+] = [e^-] + [A^-] \tag{13}$$

and the equation sets 5–8, or 10–12, can be solved with little problem, simulating the build-up of charged particle concentrations when the system starts from zero and approaches steady state in small-time increments. While doing this is instructive, and relevant examples of it will be shown later, such an approach does not (in a rigorous sense) represent the real system. In a real (pulse) system, charge is withdrawn from time to time and the system is disturbed. Clearly, eqn. 13 will be violated at this time because of the very much higher mobility of the light electrons vis-a-vis the heavy cations and anions. However, this violation must be limited on account of electrostatics: if *only* electrons were withdrawn for some (a very short) time, the remaining positive space charge would stop any further electrons from being collected. (Experimentally, this has been clearly demonstrated by the fact that the *reversed-* field phase of a.c. in the same Varian detector does *not* collect appreciable numbers of electrons, at *any* frequency of the accessible 0–10^5 Hz range[18]). Furthermore, the system has the opportunity to re-establish or at least to re-approach internal electrical neutrality during the field-free interval between pulses, particularly when this interval is long. For these reasons, eqn. 13 can be used as a (however approximate) condition incumbent on the numbers of charged particles in the simulations of this study, in which questions concerning the kind and extent of charge withdrawal become crucial.

The early ECD literature (and much of the current one, too) focusses almost entirely on the withdrawal of *electrons*; and the role the much heavier and therefore much slower cations and anions play is either ignored or treated without reference to their speed of collection.

How fast *can* these charges be collected? If we assume a fairly typical system using nitrogen at ambient pressure and 280°C, with pulses of 100 V amplitude, it will take electrons about 1 μs and typical cations and anions about 4000 μs to drift 1 cm (this is based on data from the literature[19,20], assumes unimpeded charged particles migrating through a linear field gradient, and excludes possible perturbations due to carrier gas flow, ion diffusion, etc.).

A pulse regime with 100-V, 1-μs pulses fired every 1000 μs is not atypical for ECD. Such a pulse regime would imply that a cell can be cleared of electrons by one pulse (under idealized conditions as described above), but that it would take 4000 such pulses (or 4 s in all) to produce a 1-cm drift for heavy ions. This is a disturbingly long time, even when compared with the slow elution of a gas chromatographic peak.

The early ECD literature did indeed assume that the concentration of cations in a detector was about a thousandfold higher than that of electrons but it could not sustain this position: the value of the cation–electron concentration ratio, as then perceived, gradually decreased with time and further developments of ECD theory. Following ion measurements with ECD-like sources coupled to mass spectrometers[21], the current belief evolved that positive and negative charge concentrations were, in fact, close to being equal (the latter position conforming, of course, to arguments based on simple electrostatics).

If positive and negative charge concentrations are indeed comparable, then the question immediately arises why current is observed at all or, differently phrased, how the very slow positive ions can be collected within a reasonable timeframe under a pulse regime that hardly collects the electrons. A reasonable answer, to quote Grimsrud and co-workers[22], hat "the positive charge created in the cell by electron removal tends to dissipate itself by space-charge driven migration to all grounded surfaces of the cell during the period between pulses". Of course, most cations are close to the radioactive foil anyway[12] and, given electrical field gradients not far below those imposed externally by the pulse, most have a good chance of being collected within a few (or perhaps even one) pulse interval. Hence, an adequate ion collection system appears to be in place for electrons and cations.

The fate of anions

However, the situation is different for anions. Under typical pulse conditions, anions are created mainly where most of the electrons are, *i.e.* close to the radioactive foil. Excluding removal by ventilation, or diffusion to a conducting surface, the fate of stable anions can only be neutralization by cations or, after a longer trip, neutralization by the anode. The literature, save for some of our own work, presumes almost exclusively the former. There is no question that such neutralization occurs, but we believe that it does not have to be exclusive and, in fact, we have on occasion used a space charge of anions migrating through detector region essentially devoid of cations, thereby excluding neutralization[8], to rationalize hypercoulometry (of the first kind).

The presumption of nigh exclusive anion neutralization is not totally un-

reasonable, though. The early literature had suggested that "recombination [of cations and anions] occurs 10^5–10^8 times faster than the recombination of free electrons and positive ions" and that "in a conventional electron absorption detector purged with inert carrier gas, the positive ion concentration may be several thousand times greater than the free electron concentration"[14]. Under such conditions, there would not have been any need to worry about the fate of anions: they would have been speedily consumed, providing in the process a convenient explanation for the response observed, *i.e.* for the drop in current typical of ECD signals.

As Siegel and McKeown[21] have pointed out, however, rate constants for recombination and neutralization can be expected to be of a similar order of magnitude. In fact, two passing comments that we are aware of, suggest that the apparent recombination constant in an atmospheric pressure ionization-mass spectrometry (API-MS) source —which can be made to resemble closely an electron-capture detector— could even be higher than the apparent neutralization constant[23,24]. A recent study of ours, which used the small-volume Varian detector and an SF_6–N_2 system, found, in that particular case, the apparent recombination rate constant to be almost two orders of magnitude larger than the apparent neutralization rate constant[11]. Under such circumstances the fate of anions becomes the subject of intense interest.

This is so because, under conditions where anions are incompletely or not at all collected, an ECD system can produce gas-phase amplification of response (meaning that, upon introduction of analyte, electrons would be consumed at a higher rate than the rate of the electron-capture reaction and, if hypercoulometry is indeed to exist, also higher than the rate of analyte introduction). A short discussion may demonstrate why. In this discussion we shall compare an analyte-free ("clean") system with an analyte-containing ("doped") one. The difference between the two, obviously, represents detector response.

Let us thus compare three homogeneous systems. The neutralization rate constant is imagined in the first system to be much larger, in the second equal, and in the third much smaller, than the recombination rate constant. If an electron-capturing substance is introduced into each of these three systems, the following changes will occur.

(a) When analyte enters the first system, characterized by $k_N \gg k_R$, the number of charged particles will *decrease* rapidly, since the latter is now controlled by the much faster neutralization reaction. Given that (on a molecular basis) each molecule can capture only one electron (and barring anion–neutral recycling and/or the formation of electron-capturing products), the maximum response that can be obtained is coulometric. (In fact, "$k_N \gg k_R$" would appear to be almost a precondition for analytically useful "gas-phase coulometry").

(b) When analyte enters the second system, characterized by $k_N = k_R$, the number of charged particles will essentially *stay the same*. The maximum response could also be coulometric (or, as will become evident later, slightly hypercoulometric), provided the sensing mechanism responds not to charged particles in general, but to electrons only. (If the sensing mechanism would, say, recognize *all* charged particles, response would be essentially zero.)

(c) When analyte enters the third system, characterized by $k_N \ll k_R$, the number of charged particles will *increase*: while the concentration of electrons will fall, the

concentrations of anions and cations will rise. Given the presence of a suitable measurement regime, this system is inherently capable of gas-phase amplification, hence hypercoulometry.

The reason for this is a follows: if the system does *not* collect anions, their concentration will have to continue to grow. If not limited prematurely by the cell's time constant (ventilation), anions will increase in number until their rate of neutralization will equal their rate of formation. Thus, the anions present in the system may originate from many measurement cycles, while the electrons (given their complete collection by each pulse) originate from only one. Since the system maintains essential charge neutrality, pulses will leave uncollected comparable numbers of cations and anions. (As will be seen later, the simulation system adheres strictly to that condition while the real-life system only approximates it.) The cation population will thus continue to increase over many measurement cycles commensurate with that of the anions. Whereas under analyte-free (clean) conditions electrons encounter cations not (much) larger in number than their own, they find present many more (residual) cations when the system is doped with analyte. Consequently, electron–cation recombination rates will be much higher in the doped system than in the clean one, and this larger loss of electrons (on top of the direct loss from the electron-capture reaction itself) represents what we chose to call gas-phase amplification. If conditions are right, this internal amplification can be observed externally as hypercoulometric response.

Hence, a rather surprising conclusion is reached: in a system subject to *homogeneous* kinetics, the neutralization constant must be smaller than the recombination constant in order to produce amplification and hypercoulometry. We shall refer to this type of hypercoulometry as being "of the second kind", in order to differentiate it from the type of hypercoulometry ("of the first kind") based on *non-homogeneous* kinetics[8].

(It may be noted that hypercoulometry of the *first* kind is not subject to the $k_N \ll k_R$ condition. What happens there is that the neutralization of anions is impeded primarily by their spatial separation from cations. A *low* neutralization rate constant, while enhancing the effect, is not truly required.)

Gas-phase amplification and hypercoulometry of the second kind can therefore take place only under three concurrently valid conditions: a neutralization constant that is lower than the recombination constant, a suitable measurement regime, and little or no anion collection. As regards the first, the two rate constants derived earlier[11] differ from one another by almost two orders of magnitude in the desired sense (note that these are "apparent" constants and that they may therefore include contributions from any type of *heterogeneous* response mechanism). As regards the second condition, the effect of measurement regimes can best be appreciated later in this study on hand of simulated response profiles. That leaves the third condition, the lack of anion collection, to be discussed in some detail.

At first sight, it might appear peculiar that a system capable of collecting cations should fail to collect anions. After all, the distance anions have to travel from generation to collection is, on the average, only a few times longer than the one for cations. However, this argument neglects the pronounced electrical anisotropy of the detector, as well as the typically quite weak polarization regime. In nitrogen, conventional pulses imposed on the Varian electron-capture detector collect only a fraction of available electrons (see later). Given that the mobility of anions is three to

four orders of magnitude lower than the mobility of electrons, there is little chance that any significant number of anions (unless they are formed very close to the anode) will be collected by the pulses. Certainly, anions created deep inside the radioactive cylinder will not.

Yet, could the anions perhaps reach a conducting surface during the much longer, field-free interval *between* pulses? The point was made earlier that during the field-free interval there exists, and slowly dissipates, a net *positive* space charge[22]. This charge must, if anything, *impede* the migration of any negative species. Thus there exists no effective mechanism by which anions can be removed from the system, save by the (relatively slow) process of neutralization.

Simulation parameters

For simulating an asymmetric, low-volume ECD system, we shall therefore assume as a first approximation —based on the space charge effects outlined above— that anions stay in the system until they are neutralized by cations. (This condition will be modified for a number of later simulations, but then only to demonstrate what happens when small percentages of anions *do* get collected.) We shall further assume that cations are collected relatively fast, say within one or two pulse periods.

To make the initial simulation algorithm as simple as possible, we shall indeed invoke scientific license by specifying that cations be removed, together with electrons, by a *single*, infinitesimally short pulse. (A more complex removal algorithm could be developed without too much difficulty; however, for the point we like to make here this does not appear obligatory.) The neutrality constraint (eqn. 13) demands that the numbers of collected cations and electrons be equal in this procedure.

The next question is how to enter the analyte into the simulation. The answer depends, to a significant extent, on whether one wants to deal with a weak or a strong electron capturer, a "tubular flow" or a "stirred" reactor configuration, and a sharp or a broad peak.

A weak electron capturer can be most easily simulated by a steady concentration of analyte in the carrier gas stream. A strong capturer can be treated in a rigorous manner by the use of eqn. 8 (given a perfectly stirred reactor) or it can, if it is present only in small amounts, be approximated by the use of eqn. 9. In this study, both approaches will be used. Weak capturers, being of much less interest to us, will be at first ignored.

If the strong capturer is introduced into a *tubular-flow* reactor (no longitudinal mixing), an initial concentration with no further input of analyte is entered into a moving volume element, and that element is followed by simulation of its passage through the detector. On a time-resolved basis, the result from one volume element is than combined with the results from all concurrently operating volume elements. If the strong capturer is introduced into a *stirred* reactor, the analyte input continues throughout the run. The tubular flow terminates at the end of the tube, *i.e.* at a predetermined time. The stirred reactor either reaches steady state (when the anion input rate equals the anion neutralization rate) or its approach to steady state is cut off at a predetermined time. Both system have their advantages. The Varian detector represents, in our opinion, more a tubular flow system than a stirred reactor (which maked good sense in terms of reducing its effective volume for use with capillary columns). On the other hand, stirred-reactor systems are more commonly used in ECD

theory and, in an attempt to stay within conventional bounds as far as possible, the simulations of this study will use the stirred-reactor approach.

This leaves the question whether analyte is to be introduced as a constant flow or as a Gaussian concentration profile. A Gaussian peak is not difficult to simulate, but a constant level can serve as well, provided the attainment of a steady state or predetermined cut-off is short on the timescale of the chromatographic peak. Gas chromatographic peaks vary in width from about 1 s to about 1 min. At the peak apex, the change in concentration is relatively slow, so that it can be considered constant for a calculation that does not extend beyond, say, a few tenths of a second. Therefore we shall use the simpler *constant* introduction mode in most simulations, and add Gaussian inputs only for the sake of completeness at the end of this study.

A similar reasoning applies to ventilation effects. For most qualitative purposes involving a strong capturer and a relatively short time necessary to attain steady state, one need not worry much about analyte ventilation in a stirred reactor. However, to demonstrate the relatively minor importance of the effect (and mindful of the ease of doing so), we shall be including conventional ventilation terms in a number of cases. For instance, for the ventilation of analyte molecules the term $[A]F/V$, where F is the carrier flow in cm^3/s through the detector volume V, would be added to the right side of eqn. 8. One can add similar terms to the respective equations for *charged* particles (this is commonly done in the literature and we have on occasion followed suit in this paper, simply to show that it causes only minor changes in the results), but the practice seems incongruous in a system where the movement of ions and electrons is strongly influenced if not absolutely governed by the externally imposed and internally generated electrical fields.

A further term we shall essentially neglect is diffusion. In this study, the charged-particle concentrations are not spatially resolved, but such resolution would be necessary to introduce diffusion terms on top of the (generally more important) electrostatic terms. In any case, the main postulate of this study, the existence of gas-phase amplification and hypercoulometry of the second kind, will not be greatly affected one way or the other by neglecting ventilation and diffusion. (A very rough estimate of diffusion *vs.* field-induced drift of charged particles in an electron-capture detector can be found in ref. 25.)

Measures of hypercoulometry

With the simulation conditions thus set to start at the lowest level of complexity required by the purpose at hand, the question arises how to characterize the expected hypercoulometric performance of the system. Since this study is based on a kinetic approach, the *internal* rate amplification (relative electron consumption rate *versus* analyte introduction rate) should be determined (if only for conceptual or didactic purposes). We therefore define a kinetic amplification ratio (KAR)

$$\mathrm{KAR} = \frac{\frac{\mathrm{d}[e^-]_0}{\mathrm{d}t} - \frac{\mathrm{d}[e^-]}{\mathrm{d}t}}{S_A} \ \mathrm{F/mol} \tag{14}$$

based on the difference between electron consumption rates in analyte-free and analyte-containing (clean and doped) systems, with the subscript "0" denoting the

former. S_A is the introduction rate of analyte molecules; for the coulometric analyte introduction set (eqns. 10–12) $S_A = S_{A^-}$. Inserting eqn. 5 (and its equivalent for the baseline system) into eqn. 14 modifies the latter to

$$\mathrm{KAR} = 1 + \frac{k_R([M^+][e^-] - [e^-]_0^2)}{S_A} \text{ F/mol} \tag{15}$$

Since concentrations —hence rates— change *during* each pulse-free interval, the KAR values also change through the course of each cycle. The KAR values given in this study, unless stated otherwise, are those prevailing at the *end* of each pulse interval, *i.e.* at the advent of the next pulse.

The perhaps more important, because (in a real system) externally observable, measure of detector response is the hypercoulometric ratio (HCR)

$$\mathrm{HCR} = \frac{([e^-]_0 - [e^-])\, f\, \%}{100\, S_A} \text{ F/mol} \tag{16}$$

where $[e^-]_0$ and $[e^-]$ again denote the electron concentrations in the clean and doped systems at the time the electron collecting pulse is applied, f represents the pulsing frequency in s^{-1}, and % stands for the collection efficiency of electrons (set at 100% in most simulations).

The HCR is equivalent to the detector signal in F/mol. By definition, both HCR and KAR are unity at the "coulometric limit".

EXPERIMENTAL

All *experimental* measurements were carried out on a Varian electron-capture detector[17] of *ca.* 0.35-ml volume and "displaced coaxial" electrode configuration with a cylindrical ^{63}Ni foil of *ca.* 0.5-cm radius and 1.8-cm length. The detector was generally kept at 300°C, under a carrier gas flow of 1 cm^3/s through the detector. The simulations used the same volume for their stirred-reactor kinetics.

The carrier gas nitrogen (Linde, Ultra-High Purity Grade) was further purified by passing it through a moisture trap (molecular sieve 5Å) and, in turn, a heated oxygen scavenger (Supelco). SF_6 was added to the nitrogen stream from a standard of 10.1 ± 1 ppb[a] SF_6 in N_2 (Scott Specialty Gases, Gravimetric Master Grade).

The *simulations* were carried out at three different levels (and at two locations). First, very rough estimates were produced with the help of a simple pocket calculator. Second, the main body of accurate (computer-accurate, not necessarily detector-accurate) data was obtained from simulation algorithms[b] written in Fortran for a VAX-11 computer. They solved the differential equations by using a fifth order Runge-Kutta code called "DERKF" from the "DEPAC" package of differential equation solvers written by H. A. Watts and L. F. Shampine (Sandia Labs. Albuquerque, NM, U.S.A.). DERKF integrates a system of first-order ordinary

[a] The American billion (10^9) is meant.

[b] Researchers, who are interested in the VAX-11 algorithms used in this study, are invited to contact Dr. K. W. M. Siu at the Ottawa NRC Laboratory.

differential equations of the form $du/dt = f(t,u)$ from an initial to a specified point. Relative and absolute error tolerances can be adjusted, hence the solution can be obtained with the desired (computer) accuracy. The approximate derivative at the end point is also determined by DERKF. The calling program supplies the initial values of u and t as well as the subroutine that defines the differential equations to be solved. In this study, u is $[e^-]$ and $[A^-]$ (or [A]), and t is time. Third, selected calculations[a] were run on a simple but highly efficient PC spreadsheet program (Supercalc 3, Computer Associates, San Jose, CA, U.S.A.), initially in order to obtain confirmatory results for condition sets already investigated by the mainframe VAX-11. A few of the later simulations, *e.g.* the Gaussian profiles, were run solely on Supercalc 3. The legends note which system was used ("DERKF" or "SC3").

(The use of two sets of independently developed, as well as differently formulated and executed algorithms was primarily undertaken to eliminate the particular species of bugs that often manage to elude detection by avoiding to challenge the investigator's ingrained notions of internal consistency, common sense, and what the results should turn out to be. Secondarily, it made best use of the particular capabilities of these two computing systems.)

The stirred-reactor spreadsheet program uses a basic time unit (between 10 and 100 μs) with appropriate inputs of [A] (or $[A^-]$), $[M^+]$ and $[e^-]$. After calculating the extent of reaction for one time unit, new inputs are added to the residual concentrations for the next time unit. Again, the reactions are calculated and the process continues until a "pulse" removes a certain percentage of electrons (plus a commensurate number of cations), and forwards residual particle concentrations to the next cycle (pulse period). An iteration command continues the process either to a preset number of cycles (representative of a detector cell constant) or to steady state, *i.e.* to the time when the number of electrons withdrawn by the pulse does not vary by more than a given percentage (typically set around 0.003 or 0.001%) from one cycle to the next.

RESULTS AND DISCUSSION

The "no-measurement" scenario

The simplest model is one which can be neither realized nor measured, for it starts with all concentrations being nil and proceeds in the *absence* of any electrical measurement: obviously, it is designed for perceptional purposes only. We shall use it here to demonstrate, in a graphic and largely intuitive fashion, why and how hypercoulometry of the second kind can occur. Also, as will be seen later, such a model can serve as a rough first indicator of what to expect from a comparable system in the *presence* of electrical polarization.

An example of the executed model is shown in Fig. 2 in the form of charged-particle profiles, changing with time in a doped *vs.* a clean system. The model assumes that constant inputs of analyte and ion pairs commence at time zero. The analyte is instantaneously and quantitatively converted to anions (eqns. 10–12). There

[a] Researchers interested in the typical ECD spreadsheets set up for this study, are invited to contact W. A. Aue at Dalhousie University.

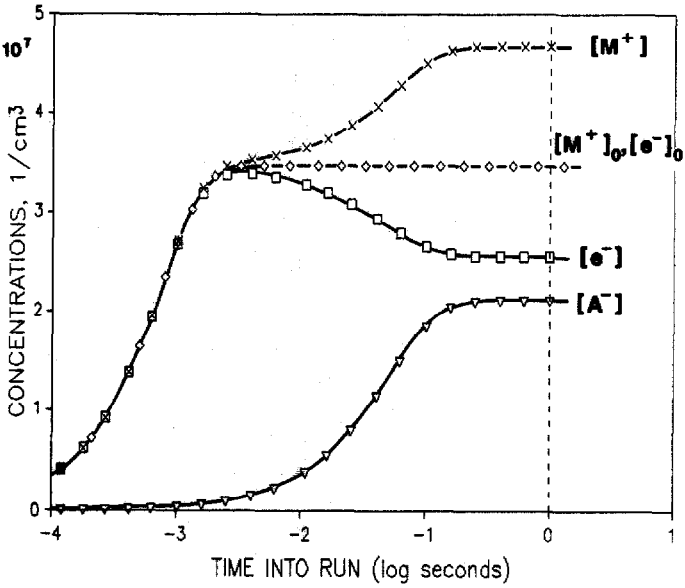

Fig. 2. Attainment of steady state in a "stirred reactor", with all concentrations starting from zero and no electrical measurement interfering. Analyte (anion) input rate S_A (= S_{A^-} = $3.57 \cdot 10^8$ $cm^{-3}s^{-1}$. Time unit for calculation: $3 \cdot 10^{-5}$ s. SC3. Full line: doped system; dashed line: clean system.

exist no means of partical removal other than recombination, electron capture and neutralization; and anions neutralized by cations do not engage in further reactions.

Under these circumstances, the cation and electron concentrations in the analyte-doped system start to build up just as they would in an analyte-free (clean) system. (The former is characterized in the graphs by solid, the latter by dashed lines.) At about 2 ms into the run, the electron concentration reaches a maximum. As the anion (and cation) concentrations continue to increase slowly, the electron concentration decreases.

The continued increase in cation concentration, and in the overall number of charged particles, is a simple consequence of the fact that the recombination constant is considerably larger than the neutralization constant. Cation and anion concentrations thus keep rising, and electron concentrations falling, until the doped system reaches steady state after about 200 ms. Thus the position of the electron maximum on the time axis is in essence determined by the recombination constant, the position of the steady state by the neutralization constant.

[Note, however, that the steady state of the classical ECD theory[14], which describes a $k_R < k_N$ system, is determined by the *recombination* constant, *i.e.* that steady state is assumed by that theory to be reached in about 1–2 ms. In the present study, this position on the time axis shows only an [e^-] maximum. But it is a maximum that, given the technical limitation on practically useable pulse periods (*ca.* 10 ms), could appear like a steady state to the experimentor. The simulation knows of no such limitation and can therefore point out that the "true" steady state is reached only after a roughly hundredfold longer timespan.]

The level of analyte introduced in Fig. 2 is taken, as are several other data in this study, from experimental work[11]. Most analyte levels are relatively high, *i.e.* they generally lie at the upper end of the (simulated) linear range or just beyond. A large amount of analyte was deliberately chosen here to demonstrate the behaviour of the system in a clear and visually unambiguous manner. However, a large amount of analyte may also mean that a substantial fraction of it is not converted to anions and will be swept out of the system. Thus the possibility exists that a system with both non-coulometric analyte introduction and strong analyte ventilation may turn out to be substantially different from the system shown in Fig. 2. The no-measurement simulation was therefore repeated, but the literature electron-capture constant for SF_6 ($3 \cdot 10^{-7}$ cm^3/s) and the experimental[11] analyte ventilation rate (carrier flow = 60 ml/min, *i.e.* $F/V = 2.86$ s^{-1}) were now used. Note that this carrier flow represents almost three detector volumes per second, a rather high setting.

Fig. 3 shows the result. If the literature capture constant is indeed applicable (*cf.* the earlier discussion) a significant fraction of analyte remains unionized. Also, the system takes a bit longer to reach steady state. These differences are to be expected. Note, however, that the steady states, *e.g.* in terms of the electron concentration, are not that far apart. They would be expected to move even closer with smaller analyte amounts, slower carrier flow, and/or a larger electron-capture rate constant. In other words, neglecting ventilation and converting a very strong electron capturer instantaneously to anions[11] produces the same qualitative scenario and would therefore appear to represent a tolerable simplification under appropriate gas chromatographic conditions.

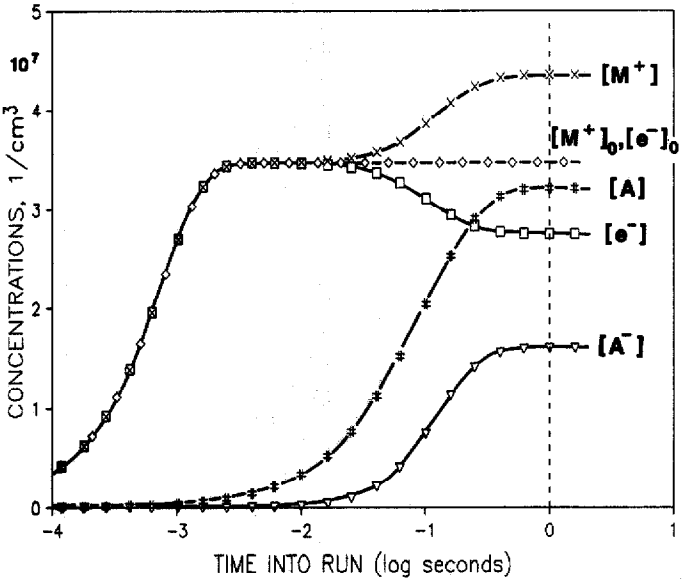

Fig. 3. Similar to Fig. 2, but $k_C = 3 \cdot 10^{-7}$ cm^3/s and analyte ventilation rate $F/V = 2.86$ s^{-1}.

Variation of measurement regimes

What is needed to use this scenario, obtain external response and achieve gas-phase amplification, is an electrical regime that removes from time to time some or all of the electrons (as well as an equal number of cations); leaving behind the anions (and, again, an equal number of cations). The next build-up of electrons will then occur in the presence of additional cations, *i.e.* recombination will occur at a faster rate. This increase in (average) recombination rate will continue from cycle to cycle until it becomes constant when the system reaches a steady state. (Note that this is a slightly different type of steady state than the one resulting from the no-measurement regime discussed above.) In order to take full advantage of this accelerated recombination (*i.e.* to obtain the largest difference in collected current between clean and doped states) the sampling of electrons and cations will likely have to occur in a time frame commensurate with this build-up of electrons.

This can be easily confirmed by simulation. The system is asked to start from the same (imagined) zero state and, at the end of every pulse period, to remove all the electrons and an equal number of cations. Anions stay in the system until they are neutralized. The numerical solutions to the simultaneous equations are obtained repeatedly until steady state is reached, that is until —in practice— successive ion concentrations no longer differ by more than a negligible percentage. Fig. 4 gives three examples of single cycles from a 1-ms pulse regime: the 1st (start), the 31st (intermediate), and the 511th (steady state) cycle. The same, relatively high analyte input is chosen for comparability and accentuated illustration. Eqns. 10–13 are used, ventilation effects are neglected. The sequence clearly shows how the rising anion level "lifts" the cation profile: the increased concentration of cations implies higher cation–electron recombination rates, hence higher response.

In order to compare such data from a pulse regime with the electrically undisturbed development of a steady state (as in Fig. 2), the end-of-cycle ion concentrations of the former, *i.e.* the ion concentrations that are reached just before charges are collected, are plotted *versus* time. This is shown in Fig. 5 for a direct comparison with Fig. 2. Note that the initial rise in ion concentrations does not appear: the graph can start only with the harvest of the first pulse. As expected, both cation and electron levels are somewhat lower in Fig. 5 than in Fig. 2. However, the important difference between electron concentrations in the clean (dashed line) and doped (solid line) systems, which corresponds to response in a detector, remains almost the same when calculated as a percentage of the baseline current for measurement and no-measurement scenarios.

Turning to other pulse regimes does not change that situation to any significant extent. Figs. 6 and 7 show plots of ion concentrations under 0.3- and 3-ms regimes (these were done on the Ottawa mainframe, with a higher accuracy than the Halifax spreadsheet run on a 30-μs time unit). The faster the pulsing, the lower are obviously the cation and electron concentrations. The concentration of anions, on the other hand, increases with the speed of pulsing (due to their slower neutralization by the now less frequent cations).

To return to the 1-ms regime shown in Fig. 5, the spreadsheet was instructed to keep a running account of internal and external response amplification, *i.e.* KAR and HCR values. The point was made before that these must increase and finally become constant as the system moves to steady state. Fig. 8 shows the profiles, which rise

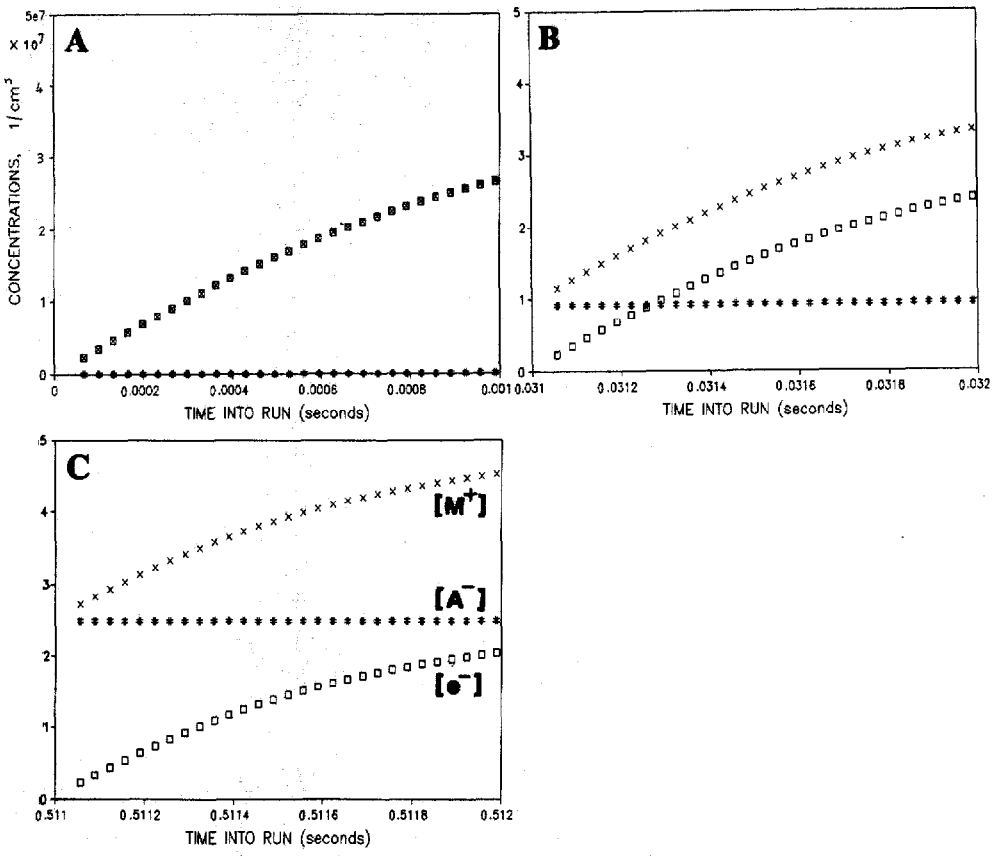

Fig. 4. Ion concentrations under a 1-ms measurement regime, during the "field-free" periods of three cycles (between pulses that remove 100% of electrons, 0% of anions, and cations commensurate with electrical neutrality). Analyte (anion) input rate S_A (= S_{A^-}) = $3.57 \cdot 10^8$ $cm^{-3}s^{-1}$. A: start (cycle No. 1), B: intermediate (cycle No. 31), C: steady state (cycle No. 511). Basic time unit: 30 μs. SC3. × = Cations; □ = electrons: # = anions.

clearly above the coulometric limit (F/mol = 1). Internal gas-phase amplification and external hypercoulometry are both prominently displayed by the simulated system. In other words, hypercoulometry of the second kind *is* possible. The KAR and HCR values are so high that even fairly large errors introduced by the varous assumptions would not question their existence.

The HCR and KAR profiles do not coincide, but neither would they be expected to (that KAR and HCR are equal at steady state in Fig. 8 is incidental). Their difference stems from the fact that the internal KAR defines a ratio of rates at a particular moment in time (in Fig. 8: just before the pulse), while the external HCR measures the electron concentrations (as they have built up to the moment the pulse strikes) and converts them to a response integrated over time. Also, as will be seen later, KAR and HCR reach their maximum values at different pulsing frequencies.

Further, KAR values must change within each cycle, since the analyte introduction rate remains constant but the cation and electron concentrations do not.

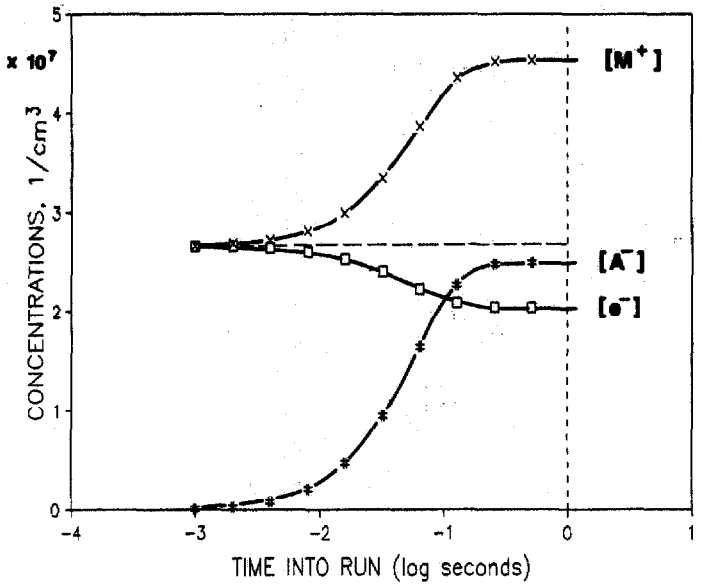

Fig. 5. End-of-cycle ion concentrations under a 1-ms measurement regime. Conditions and symbols as in Fig. 4.

Fig. 9 shows such KAR variation *within* one steady-state cycle (the same cycle, incidentally, whose ion concentrations are depicted in Fig. 4C). The KAR maximum is diagnostic in semiquantitative fashion: one could reasonably expect that a pulse interval close to 0.6 ms would have produced higher end-of-cycle KAR values in the graph of Fig. 8.

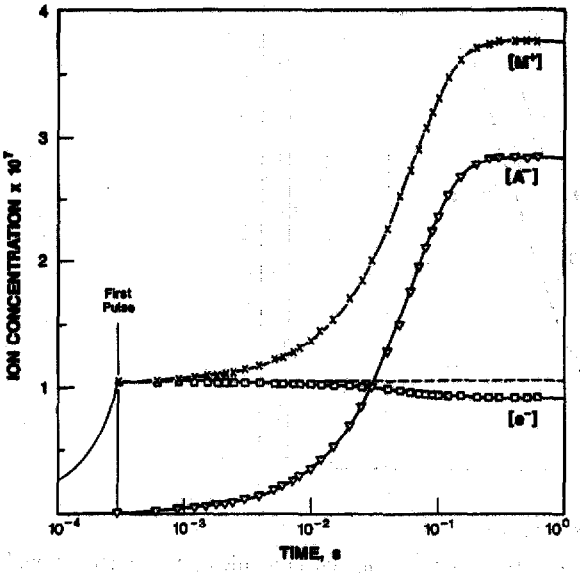

Fig. 6. Similar to Fig. 5, but under a 0.3-ms measurement regime. DERKF algorithm.

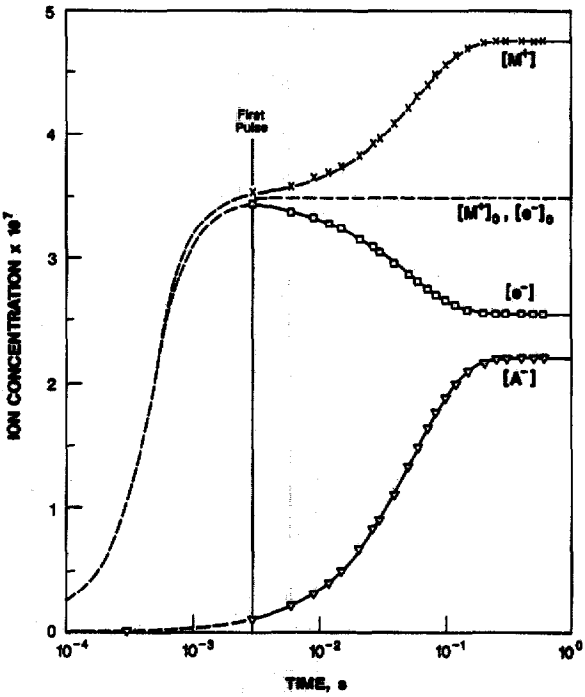

Fig. 7. Similar to Fig. 5, but under a 3-ms measurement regime. DERKF.

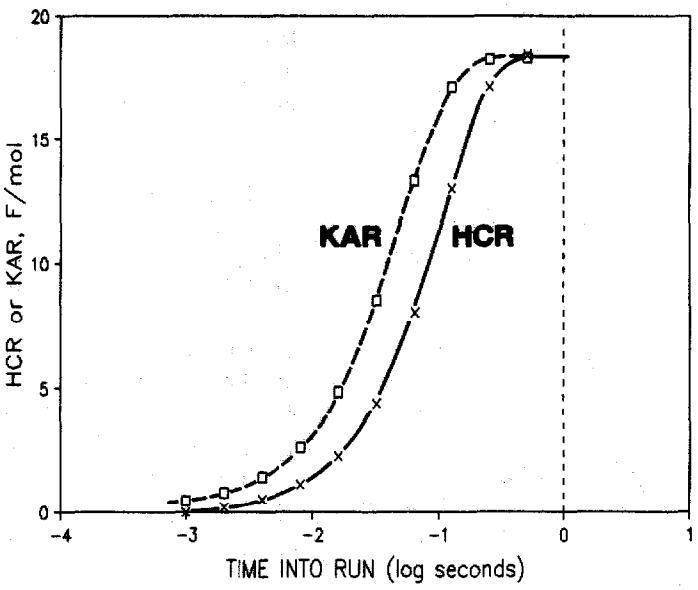

Fig. 8. Hypercoulometric ratio (×) and end-of-cycle kinetic amplification ratio (□) during the attainment of steady state. Conditions as in Figs. 4 and 5.

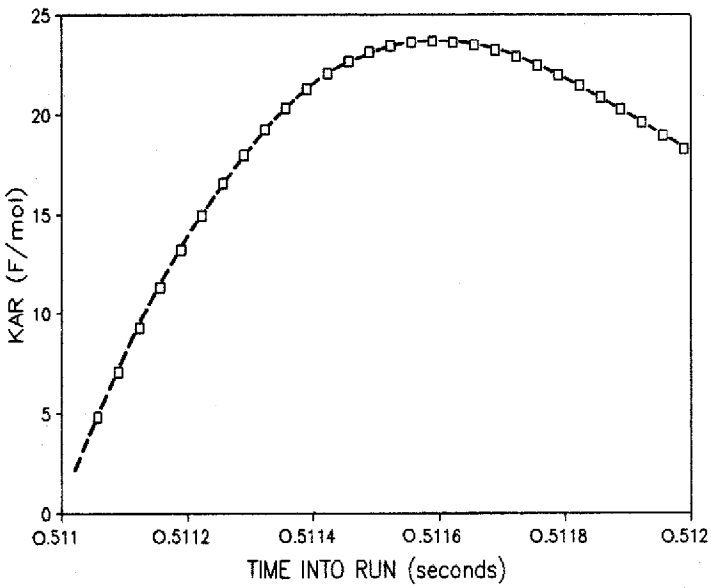

Fig. 9. Kinetic amplification ratio during a steady-state cycle. Conditions as in Fig. 4C.

Figs. 2–9 are typical examples selected from a larger number of different "start-from-zero" simulations, which were run (on two different computer systems) for different pulsing frequencies (including zero), different analyte inputs, different ventilation conditions, etc. They all conform, *mutatis mutandis*, to the general descriptions and interpretations given above.

While the start-from-zero simulations provide a firm basis for assessment of factors involved in ECD response, as well as for an intuitive understanding of the process, they are found wanting in one crucial aspect: a real-life ECD does not, like the model, start from a condition where all concentrations are zero. In particular, it does not experience a sudden jump in analyte input from zero to a high, constant level. Gas chromatographic peaks are very rarely sharper than a few seconds (and very rarely broader than a few minutes). Thus, if we take the highest point of a peak as the point of calculation, a very similar analyte input must have persisted for the preceding few tenth of a second. But that means, if the timeframes of attaining steady state in Figs. 2–7 are any indication, that the strong electron capturer of this system keeps most of the time, and particularly when it counts, at or near *steady* state.

Differently expressed, if the concentration profile of a peak develops slow on the timeframe it takes the kinetics to reach steady state, then calculations using only the steady state will adequately represent the system. Clearly, the validity (closeness) of this approximation will depend on a variety of conditions, notably the carrier flow through the detector, the width and height of the chromatographic peak, the magnitudes of k_C and k_N, etc. Also, it will depend on the *a priori* features of the model, *i.e.* the resistance of anions to be collected or be swept out of the system, and the appropriateness of the assumed electrical neutrality and stirred-reactor formalisms.

For the primary purpose of this study —to demonstrate that hypercoulometry of the second kind can actually exist and, furthermore, to describe its behaviour under

various experimental conditions— small (or indeed, since the effect is so large, quite sizeable) errors in KAR and HCR would not really matter. We shall therefore follow the most expedient route by calculating from steady states only. However, we shall need to keep in mind that calculated HCR values may thus come out too high in comparison with experimental ones; and that the effects of sharp peaks, fast ventilation, less than complete anion retention, etc., might need to be taken into account in any treatment aspiring to greater accuracy.

The easiest way to portray the steady-state performance under *different* measurement regimes is to plot the maximum ion concentrations, kinetic amplification ratios and hypercoulometric ratios *versus* the pulse period. (Note that "pulse period" is the expression commonly used in the ECD literature for the cycle time. Since the simulation uses infinitesimally short pulses, the pulse period and the pulse interval become numerically equal in this study.) For each pulse period, the algorithms determine the steady-state concentrations by using the iterative approach exemplified in Figs. 6 and 7. KAR and HCR values are then easily calculated from a steady-state cycle according to eqns. 15 and 16.

An example of such a summary of calculations is given in Fig. 10. Note that here, despite the visual similarity, the ion concentrations do not "develop in time" as they did in earlier plots; but that the data characterize only the steady states, *i.e.* the final, constant values derived by *separate* iteration for each pulse period setting.

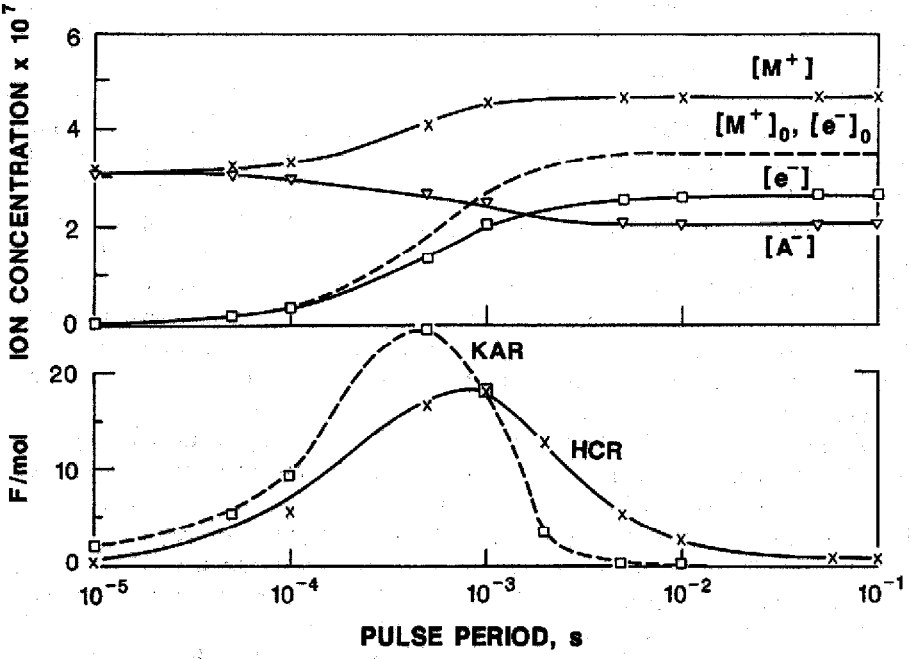

Fig. 10. Ion concentrations and HCR/KAR values at steady state under different pulsing regimes. DERKF. Analyte (anion) input rate $S_A (= S_{A^-}) = 3.57 \cdot 10^8$ cm^{-3} s^{-1}. Top: × = Cations; □ = electrons; ▽ = anions (all in doped system, full lines); cations and electrons in clean system: dashed line. Bottom: × = HCR (full line); □ = KAR (dotted line).

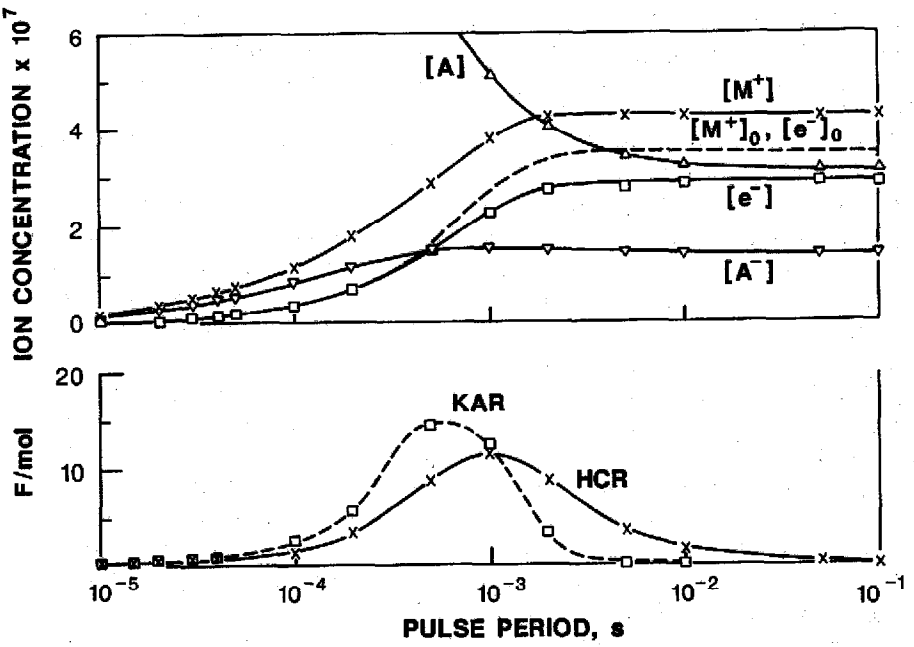

Fig. 11. Similar to Fig. 10, but $k_C = 3 \cdot 10^{-7}$ cm^3/s and all-particle ventilation rate $F/V = 2.86$ s^{-1}.

The end-of-cycle KAR profile is higher, and occurs at a shorter pulse period, than the HCR profile. This, as alluded to earlier, is a consequence of the fact that KAR is differential while HCR is integral in character. The maximum HCR value, the counterpart of which in a real-life system represents an easily measured quantity, is 18 F/mol. (The anion input in this particular demonstration case is beyond linear range; HCR values *within* linear range are still higher.)

It is obvious, however, that the use of eqns. 10–12 and the absence of ventilation may have produced unrealistically high KAR and HCR values. The simulations were therefore repeated, but eqns. 5–8 were used with ventilation terms of 2.86 s^{-1} and an electron-capture rate constant of $3 \cdot 10^{-7}$ cm^3/s. The result is shown in Fig. 11.

(This process is similar to the earlier check on system variability involving Figs. 2 and 3; and the foregoing *caveats re* data applicability pertain here as well. Note also that, in contrast to Fig. 3. Fig. 11 goes one step further by attaching conventional ventilation terms not only to neutral but also to all charged particles. This may not have a basis in reality. However, the objective here is not to describe the "true" state of the ECD (we have no reasonable means of doing so in these *a priori* calculations), but to define two extreme positions that, we hope, will bracket reality.)

In Fig. 11, the position of the KAR and HCR maxima on the time axis has not noticeably changed, but the maxima are now clearly lower. The maximum HCR value has declined by about one third (compare this to the decline in the electron concentration by about one fourth among Figs. 2 and 3). Note that a comparative run (not shown here) with the same electron-capture constant but *without* ventilation

produces KAR and HCR profiles very close to those of Fig. 10: the decrease in response is therefore mainly due to the use of the large and exhaustively applied ventilation terms, as opposed to the use of the finite (but relatively high) capture constant. As one would expect, the finite capture constant makes for a dramatic change in anion (and cation) concentrations only at very short, and analytically irrelevant, pulse periods.

Even under such flushing conditions, the simulated HCR values still reach a maximum of about 12 F/mol. In other words, hypercoulometry of the second kind is still clearly present. Note that in the earlier cited experimental study[7], the highest measured HCR values were 8.0 F/mol for CCl_4, 3.7 for SF_6 and 5.0 for lindane.

(One of the reviewers of this manuscript brought to our attention that a recent flowing-afterglow study[26] had found a high electron-capture rate for the CCl_3 radical. While this is of no consequence to the present context, it is interesting to note that the ECD response of CCl_4 (as that of certain, more complex strong capturers[27], is likely to contain a significant contribution from a reaction product.)

In the absence of *experimental* information on the extent of ventilation of *charged* particles, as well as of the apparent value of k_C in the model detector, this study seems to have gone as far as it can in demonstrating the existence of hypercoulometry within the boundaries of previously determined or at least plausibly derived parameters. We shall therefore go one step further and explore other aspects of system ruggedness, by observing how the simulated system would respond to changes in (a) the neutralization and recombination rate constants; (b) the anion collection rate; (c) the cation and electron removal efficiency; and (d) the type of analyte input (constant level *vs.* Gaussian profile). Our reason for including this "seemingly endless number of equivalent computer simulations" (as one of the reviewers of this manuscript annotated) is (a) to demonstrate that hypercoulometry occurs under a very wide range of conditions and not just under a peculiar set of circumstances, and (b) to gain an understanding of how these conditions (rate constants, pulse regimes etc.) are likely to influence the magnitude of hypercoulometry in particular and ECD response in general.

Variation of rate constants

We have demonstrated earlier on that the manifestation of a reasonably large hypercoulometric effect of the second kind requires the existence of a system whose neutralization rate constant is significantly smaller than its recombination rate constant. One might therefore ask how the ratio of the two rate constants in a homogeneous model influences the ion concentrations and, in turn, the KAR and HCR values.

It is not necessary to employ a computer for appreciating how far ion concentrations can rise with a falling neutralization rate constant. Rather, the *maximum* steady-state concentrations in a no-measurement scenario can be derived in the following manner.

Assuming that all analyte molecules are converted to anions and that there are no ventilation effects, the equation for anions at the steady state (indicated here by the subscript "s") is

$$S_{A^-} = k_N[M^+]_s[A^-]_s \tag{17}$$

It can be modified by inserting the value for $[A^-]$ gained from the neutrality constraint (eqn. 13) to yield

$$S_{A^-} = k_N[M^+]_S^2 - k_N[e^-]_S[M^+]_S \tag{18}$$

Substitution of $[e^-]$ from eqn. 10 at steady state

$$[e^-]_S = \frac{S_{IP} - S_{A^-}}{k_R[M^+]_S} \tag{19}$$

into (eqn. 18) then results in an expression for the cation concentration

$$[M^+]_S = \sqrt{\frac{S_{A^-}}{k_N} + \frac{S_{IP} - S_{A^-}}{k_R}} \tag{20}$$

which can be re-inserted into eqns. 17 and 19 to yield expressions for the steady-state anion and electron concentrations:

$$[A^-]_S = \sqrt{\frac{S_{A^-}}{k_N\left[1 + \frac{k_N}{k_R}\left(\frac{S_{IP} - S_{A^-}}{S_{A^-}}\right)\right]}} \tag{21}$$

$$[e^-]_S = \sqrt{\frac{S_{IP} - S_{A^-}}{k_R\left[1 + \frac{k_R}{k_N}\left(\frac{S_{A^-}}{S_{IP} - S_{A^-}}\right)\right]}} \tag{22}$$

Fig. 12 has been calculated via eqns. 21 and 22, with the subsequent use of eqn. 13 for the cation concentration, by varying the neutralization constant while keeping the apparent N_2 recombination constant at the same (the earlier measured) value. The position of the experimental neutralization rate constant is marked by an arrow.

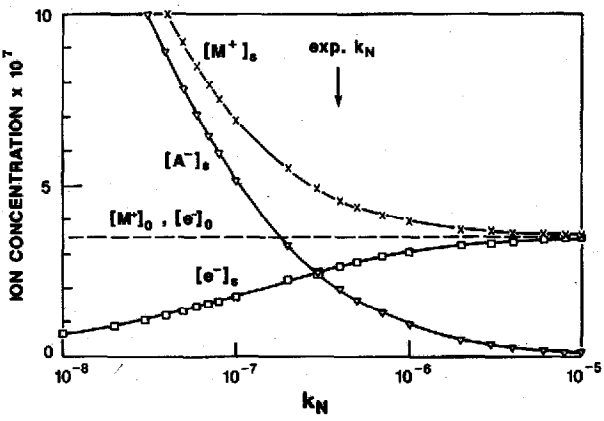

Fig. 12. Theoretical maximum ion concentrations at steady state, as dependent on the neutralization constant, with k_R at the experimental value of $2.9 \cdot 10^{-5}$ cm^3/s for SF_6.

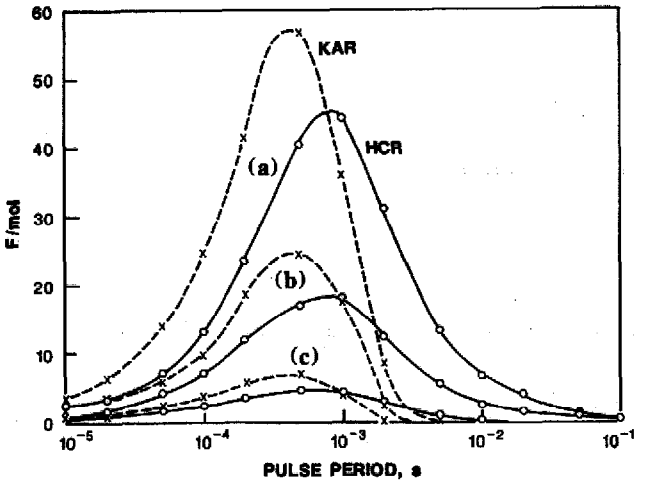

Fig. 13. HCR and KAR at different values of k_N. Anion input rate: $3.57 \cdot 10^8$ cm^{-3}s^{-1}, $k_R = 2.9 \cdot 10^{-5}$ cm^3/s. k_N = (a) $3.8 \cdot 10^{-8}$, (b) $3.8 \cdot 10^{-7}$ and (c) $3.8 \cdot 10^{-6}$ cm^3/s. DERKF only. HCR full lines, KAR dashed lines.

It is fairly obvious that relatively small changes in the ratio of the two rate constants can lead to significant differences in response. This is important, because the experimental values for these constants carry sizeable error limits[11]. These error limits are by no means large enough to call into question the kinetic concept of hypercoulometry as developed here, but they do introduce some uncertainty about just how large the effect can become.

It should also be remembered that the apparent recombination constant was experimentally determined in "pure nitrogen"[11]. That brings up two points for consideration. First, cation–electron recombination during the passage of a peak (*i.e.* in the presence of analyte, its fragments, or perhaps even a massive co-eluting but essentially non-electron-capturing peak) cannot automatically be equated with recombination in pure nitrogen. For instance, the possibility exists that some of the positive charge would transfer from N_4^+ (or other nitrogen species) to an analyte fragment. Second, and more important, minute traces of atmospheric oxygen and other contaminants are always present in conventional detectors, despite all the precautions taken to prevent them from intruding, and the experimentally apparent recombination constant is therefore likely to come out on the high side (*c.f.* ref. 11). It should be mentioned in this context that a comparison of the "best" neutralization and recombination rate constants from the chemical (not necessarily the ECD) literature shows them to be closer together than our own, experimental ones. For instance, the earlier mentioned theoretical study of non-homogeneous kinetics in a large-volume, parallel-plate detector[9] used as literature values $4.3 \cdot 10^{-6}$ and $4.0 \cdot 10^{-7}$ cm^3/s (as compared with the detector-derived apparent constants of $2.9 \cdot 10^{-5}$ and $3.8 \cdot 10^{-7}$ cm^3/s) for k_R and k_N, respectively.

The ion concentrations of Fig. 12 are those of an electrically undisturbed (no-measurement) process. However, a comparison of the values obtained from it (by using the experimental neutralization rate constant for SF_6, $k_N = 3.8 \cdot 10^{-7}$ cm^3/s), with some of the detector simulations using a 1-ms drive regime, a setting that is not too

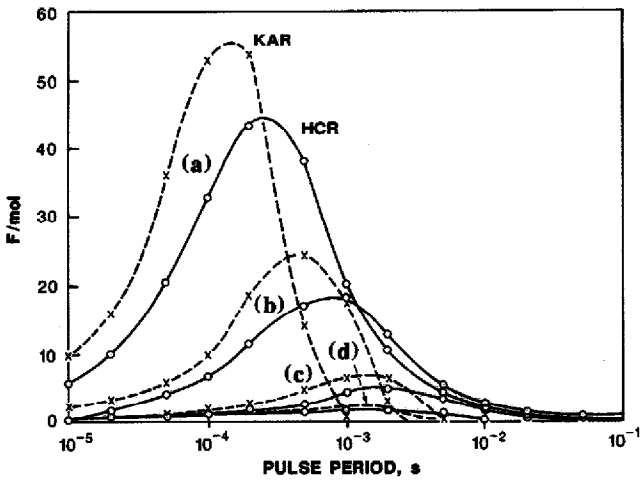

Fig. 14. HCR and KAR at different values of k_R. Anion input rate: $3.57 \cdot 10^8$ cm^{-3} s^{-1}, $k_N = 3.8 \cdot 10^{-7}$ cm^3/s. k_R = (a) $2.9 \cdot 10^{-4}$, (b) $2.9 \cdot 10^{-5}$ and (c) $2.9 \cdot 10^{-6}$ cm^3/s. Additional case (d) $k_R = k_N = 3.0 \cdot 10^{-6}$ cm^3/s. DERKF only. HCR full lines, KAR dashed lines.

far from the optimal one, shows that the two sets do not differ much. Still, it is worthwile to check, by simulation, what would happen to KAR and HCR values over a broad range of frequencies, if one or both rate constants were changed. Since only trends and comparability matter in this case, the relatively high anion input rate of $3.57 \cdot 10^8$ cm^{-3} s^{-1} (as used in most graphs) is maintained, and the profiles of Fig. 10 are included for comparison. The results are shown in Figs. 13 and 14.

Fig. 13 uses the experimental k_R value, and varies k_N by one order of magnitude up and down from the experimental constant. The k_R/k_N ratios are 7.7, 77 and 770. Note that the maxima stay at the same pulse period. Fig. 14, on the other hand, keeps k_N at the experimental value and varies k_R one order of magnitude up and down. Also included is one case in which the two constants are equal. The ratios are again 7.7, 77 and 770 (as well as 1). With the change in recombination constant, however, the position of the maxima changes. The reason seems clear: the faster the cation–electron recombination proceeds the faster must measurements be taken to let the system remain atop the response maximum.

The profiles of Figs. 13 and 14 serve the purpose of pointing out trends while preserving comparability. However, they describe conditions where, particularly at low k_N values, the measurements are grossly above linear range. We therefore add (for the purist) two simulations that are deliberately kept within linear range, though now at the expense of reason: the assumptions of the model and the comparability to real-life electron-capture detector systems are being severely compromised. Fig. 15 shows the maximum HCR possible under a 1-ms pulse regime and an anion input of only $1 \cdot 10^6$ cm^{-3}s^{-1}; while Fig. 16 shows the time necessary to reach that maximum HCR (*i.e.* the time necessary to reach steady state starting from zero).

The maximum HCR for conditions involving the *experimental* rate constants is now about 50 F/mol, and the time to reach that steady state about 0.8 s. Note that decreasing the neutralization constant by a factor of ten increases both HCR and the

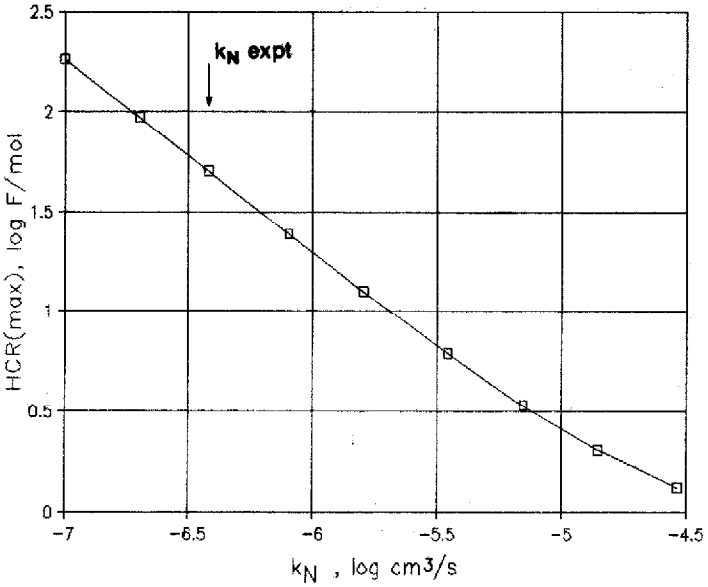

Fig. 15. Theoretical maximum HCR obtainable under a 1-ms pulsing regime at different values of k_N. Anion input rate: $1 \cdot 10^6$ cm^{-3}s^{-1}; $k_R = 2.9 \cdot 10^{-5}$. $k_C = 3 \cdot 10^{-7}$ cm^3/s; $F/V = 0$ s^{-1}, steady state. SC3 only.

time to achieve it by a factor of ten (the latter two factors are quite a bit smaller in the above-linear-range simulations of Figs. 13 and 14). The interesting aspect of these theoretical numbers is that they point to the possibility of using for analytical purposes (afar the detector realm) simple gas-phase kinetics for achieving unusually large response amplification factors. The situation is reminiscent of kinetic analysis based on catalytic effects. One could even, with some stretch of the definition that requires a catalyst not to be consumed by the reaction it accelerates, perceive the present ECD model as anions in the system "catalyzing" the recombination of ion pairs. Of course, to utilize the effect requires the ability to collect certain reacting species while leaving others behind. We are not immediately aware of any practical gas-phase system beyond the electron-capture detector that could make use of such kinetics, but the theoretical possibility certainly exists.

Before exposing the simulated detector to further ruggedness tests, we should pause to recall a earlier statement. If k_N were equal to k_R, we said, the numbers of charged particles should remain essentially the same on introduction of analyte, and the maximum response should therefore not exceed 1 F/mol. Now, Fig. 14 contains a case where k_N equals k_R, but KAR and HCR values are higher than unity! How can this system turn out to be (even slightly) hypercoulometric? Recall that the earlier statement focussed primarily on ion concentrations in a system whose development was not disturbed by electrical measurement. Under the present pulsing regime, however, electrons are removed while anions are retained. Hence, a small, residual cation population (equal to the anion population) will exist just after the pulse; and newly incoming electrons will experience a slightly higher recombination rate. Since, in this case, the anion concentration is being kept small by the comparatively high neutralization constant, the extent to which KAR and HCR can exceed unity is also quite small.

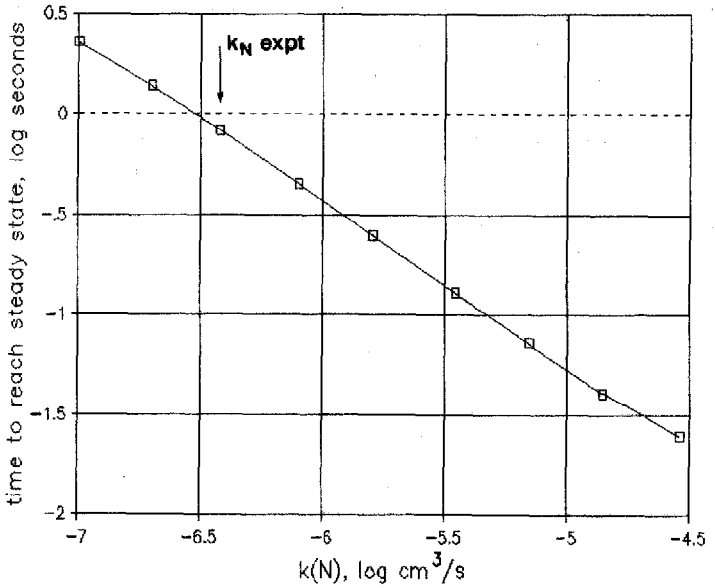

Fig. 16. Time necessary to reach theoretical maximum HCR (as shown in Fig. 15), starting from zero concentrations and at different values of k_N. SC3 only.

Anion collection

The next aspect to be scrutinized is the collection of anions by an electrode (should this process indeed occur). So far, simulations were based on the assumption that anions remain in the system, and that seemed reasonable to assume in the absence of any effective means of anion collection. However, when it takes a long time to reach steady state and when, during that time, some 10^2 to 10^3 pulses operate on the system, even a very small fraction of anions being excised by each pulse could lead to a big difference in response.

To gain an understanding of the possible magnitude of this effect, simulations are set up in which each pulse collects 1, 5, 10 or 25% of the anions present at the time. (In accordance with eqn. 13, the numbers of particles removed must be the same for opposite charges; thus the number of collected cations must equal the sum of collected electrons and anions.) Fig. 17 presents the results of this simulation together with data from a previously investigated system that did *not* lose any anions to the pulses.

Two aspects of the simulation are immediately obvious. First and foremost, even a small fraction of anions collected by each pulse results in a large decrease in response. For instance, a mere 1% of the anions removed per 1-ms cycle brings about a quarter reduction of response (under the particular conditions used). Second, the KAR and HCR maxima move to somewhat longer pulse periods as the percentage of anion collection increases. The latter effect is to be expected because the detrimental effect of anion collection on KAR and HCR values is minimized by pulsing slower, *i.e.* by collecting anions less often.

Electron and cation collection

The last aspect to be scrutinized is the electron and cation collection rate.

So far, all available electrons (and a commensurate number of cations) were collected by each pulse. Each simulation pulse was infinitesimally short and infinitely powerful: the charged particles were removed instantaneously. How close does this assumption approach reality?

It is usually presumed possible to make experimental pulses powerful and long enough to remove almost all electrons from a conventional ECD. The required pulse strength and duration depends on the nature of the foil, the dimensions and geometry of the detector, and the choice of carrier gas. In the particular commercial detector that served as the model and as the provider of apparent rate constants for this study, *i.e.* the ^{63}Ni Varian detector with nitrogen as carrier gas, such pulses needed to be far stronger than commonly used in ECD practice. For instance, it took pulses of about 100-μs width and 50- to 100-V amplitude to collect most electrons under a 1000-μs pulsing regime (many conventional detector power supplies are indeed not capable of delivering pulses above 50 V).

In contrast, the earlier study of hypercoulometry occurring in the Varian detector under essentially "field-free" conditions, employed pulses of 0.5- and 1.0-μs width and 10- to 40-V amplitude[7]. Such regimes were used deliberately to comply, in a formal manner, with the classical literature criterion of "field-free" conditions. However, using such regimes also meant that, say at 1 ms, less than a quarter of the theoretically collectable current was actually collected. Consequently, even from a point of view that would (in our opinion unjustifiedly) disregard space charges and consider only the light *electrons* (which are three to four orders of magnitude faster than the heavy cations and anions), a cursory glance at the system's response to incomplete electron collection may not be amiss.

There is, in addition, a second point of view that needs to be taken into account.

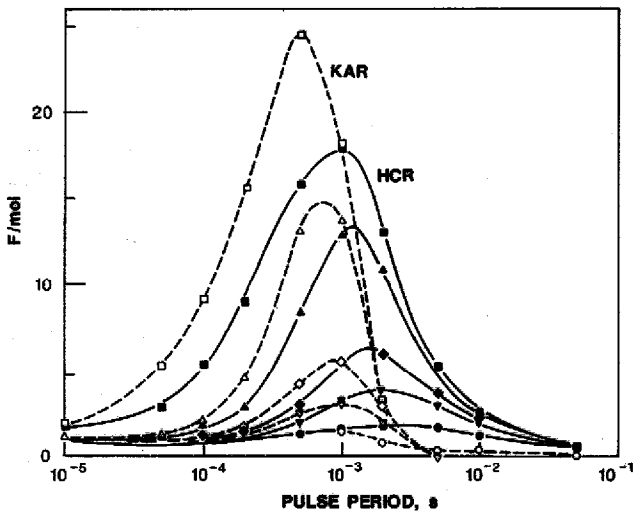

Fig. 17. Effect of anion collection efficiency on HCR and KAR values. $S_{A^-} = 3.57 \cdot 10^8$ cm^{-3}s^{-1}. DERKF only. HCR: full line, full symbols. KAR: dashed line, empty symbols. Percent of anions collected by each pulse: □ = 0%; △ = 1%; ◇ = 5%; ▽ = 10%; and ○ = 25%.

It refers to certain peculiarities of the simulation algorithms as contrasted with real-life electron-capture detectors; and it concerns *cations*.

As was recalled earlier for a real-life detector, most of the cations are driven by their own space charge to the radioactive foil and are collected there *during the field-free interval, i.e.* after the application of the pulse that removed the electrons. Hence, electrons newly entering the experimental system encounter more cations than they would in the simulated system, where pulses are infinitely short and powerful and where collection does not take place at any other than at pulse time.

Three aspects need to be kept in mind here. First, the effect of residual cations occurs both in the doped and the clean experimental system, hence at least part of the error in regard to response cancels out. Second, the experimentally determined, apparent rate constants, which are being used for the simulation runs of this study, may have part of the slow-cation-collection effect already "built in". Third, the experimental effect of delayed cation collection will be strongest at *high* pulsing frequencies, *i.e* when it becomes more difficult for the cations to disperse effectively within the short interval between pulses. In other words, such high frequency regimes are most likely to produce a (limited) charge imbalance, *viz.* $[M^+] > [e^-] + [A^-]$.

Thus the simulation suffers to some extent from the strict application of eqn. 13 and, more importantly, from the unfettered reign of its instantaneous and omnipotent pulses. On the other hand, those boundary conditions and capabilities make the pulses exceedingly convenient to use. Otherwise, the algorithm would have to incorporate some functions following the decay in the excess concentration of positive charge, as well as its effect on the collection of negative charge. That problem is one of non-homogeneous kinetics and has been solved rigorously only for an idealized parallel-plate system[9].

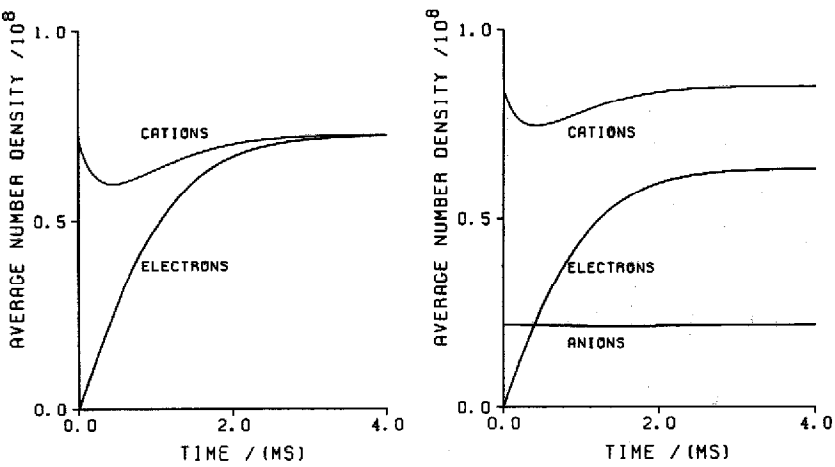

Fig. 18. Variation of the averaged ion concentrations in a simulated parallel-plate electron-capture detector during a complete pulse period at steady state. Radio-isotope: tritium, interelectrode distance: 5 mm, pulse period: 4 ms, pulse width: 5 μs, pulse amplitude: -30 V, analyte introduction rate (right graph only): $6 \cdot 10^9$ $cm^{-3}s^{-1}$. From ref. 10, which should be consulted for the rate constants, mobilities, primary ion pair distribution, and algorithms used.

Because of its general interest for this work (and beyond), Fig. 18 reproduces from the cited thesis[9] two graphs of average ion concentrations during a relatively long pulse interval at "steady state" (no further changes from one cycle to the next) in a clean and a doped system. Note that this simulation is *ab initio, i.e.* its spatially and temporally resolved ions move under the local field gradients in accord with their innate mobilities. The shorter the pulse interval, the farther does the system stray from charge neutrality. For further information, the original work[9] should be consulted; however, even taking into account that its systems and simulations are very different from those of the present study, it does offer considerable insight into the expected magnitude of deviation from electrical neutrality, and the time frame in which such perturbations are likely to subside.

The present detector system, because of its pronounced electric anisotropy, would be much harder if not impossible to handle in an equally rigorous manner. However, in terms of the response-determining electron–cation recombination rate, a less than complete electron collection (forcing a commensurately reduced cation collection) fortunately achieves a similar effect. Also, since the neutrality constraint (eqn. 13) couples the electron and cation collection rates, both can be studied by one type of simulation. The particular simulations carried out for this study assume that the collection of electrons by each pulse is 100, 70, 50, 30 and 10% effective.

The results are shown in Fig. 19 for KAR and in Fig. 20 for HCR values. The effect is small in terms of response magnitude (in fact, the HCR hardly changes) but in terms of the optimum pulse frequency it is dramatic. The fewer electrons (and cations) are removed, the farther the KAR or HCR maxima shift toward shorter pulse periods. This is perfectly reasonable when one considers the build-up of electron density, *e.g.* in a cycle as shown in Fig. 9 for a steady state. Somewhere within that cycle lies the point where KAR reaches its maximum. If we start from a zero electron concentration right

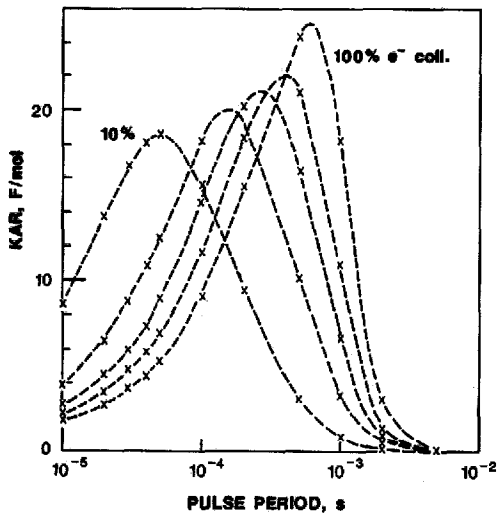

Fig. 19. Effect of electron collection efficiency on KAR values. $S_{A^-} = 3.57 \cdot 10^8$ cm^{-3}s^{-1}. DERKF only. Percent of electrons collected by each pulse, from left to right: 10, 30, 50, 70, and 100%.

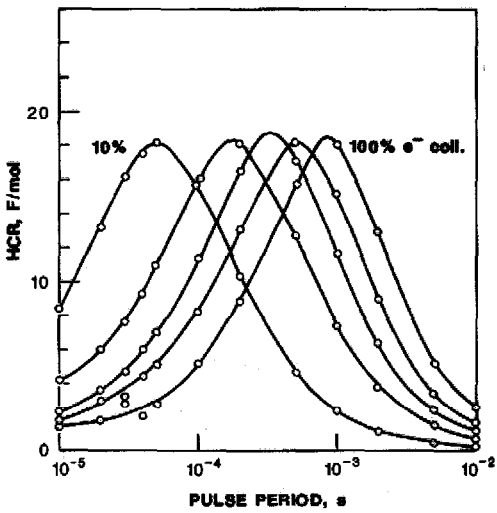

Fig. 20. Effect of electron collection efficiency on HCR values. Otherwise similar to Fig. 19. Percent of electrons collected by each pulse, from left to right: 10, 30, 50, 70, 100%.

after the pulse, that point will be reached in about 0.6 ms. However, if a certain percentage of electrons is left over after the pulse, we start already higher up on the slope and reach the imaginary KAR apex (imaginary because it may shift slightly under the new conditions) in a shorter time. In other words, the fewer electrons are collected by the pulse, the shorter will be the optimum pulse interval. Similar reasoning applies, *mutatis mutandis*, to the HCR value.

A Gaussian input

So far we have dealt only with *constant* analyte inputs, reasoning that the time necessary to reach steady state was generally shorter than significant concentration changes in chromatographic peaks. However, the spatial integrity of peaks (how well the detector signal follows the analyte input) is also of great concern to chromatographers. We shall therefore run a few simulations with Gaussian inputs.

To run a Gaussian profile in time t through the spreadsheet program, the normally constant analyte input S_A is replaced by

$$S_A = \frac{A_I}{\sigma\sqrt{2\pi}} \exp[-(t-t_R)^2/2\sigma^2] \tag{23}$$

where A_I is the amount injected (as molecules into a 1-cm^3 detector), t_R is the retention time and σ the standard deviation (both in s) of the Gaussian peak. The pre-exponential term is, of course, equal to the peak height.

Since response is strongly hypercoulometric, the signal leaving the detector would turn out to be much larger than the solute entering it (if measured in electrons and molecules, respectively). The response trace is therefore subjected to normalization such that the two curves coincide at the solute maximum also known as the analyte retention time. This means dividing all response values by a constant number, *i.e.* the

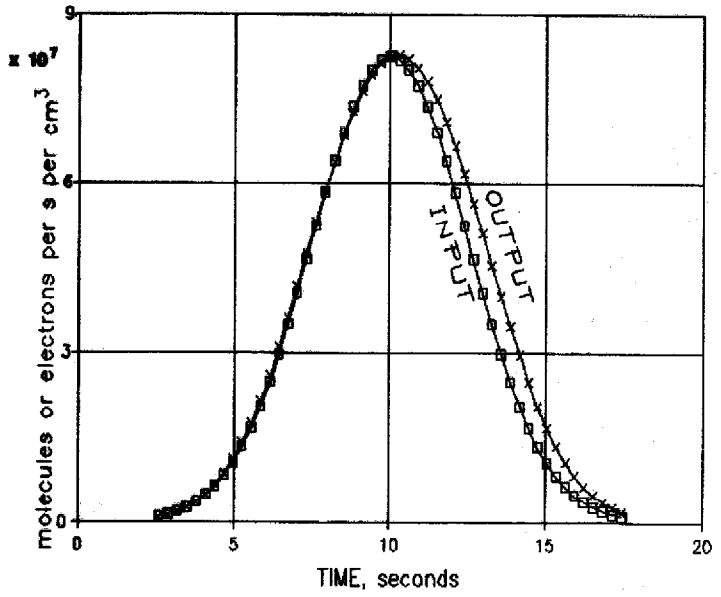

Fig. 21. ECD response (×) obtained from a Gaussian input peak (□) (t_R = 10 s, σ = 2.5 s) of 0.125 pg SF_6. The simulation uses a 1-ms pulse regime, the literature capture constant and a fast vent rate (2.86 s^{-1}) for SF_6, as well as a single amplitude normalization factor. SC3 only. See text for further explanation.

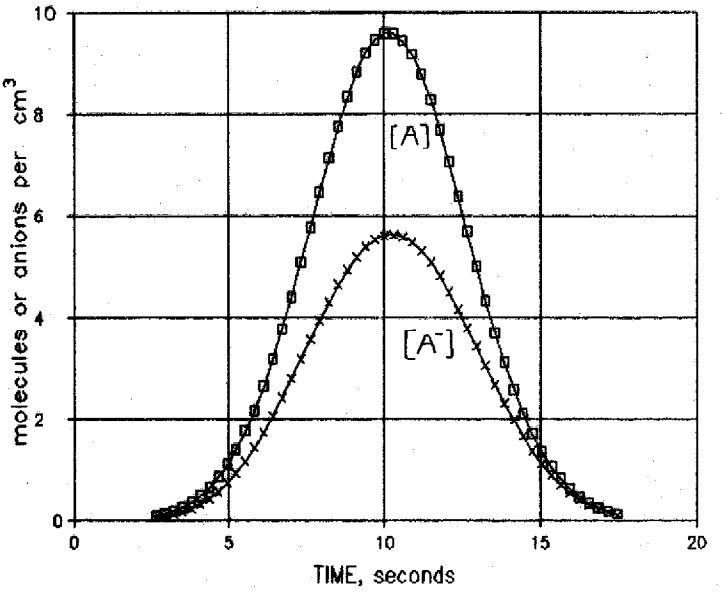

Fig. 22. Analyte (□) and analyte-derived anion (×) concentrations during the passage of the Gaussian input peak shown in Fig. 21.

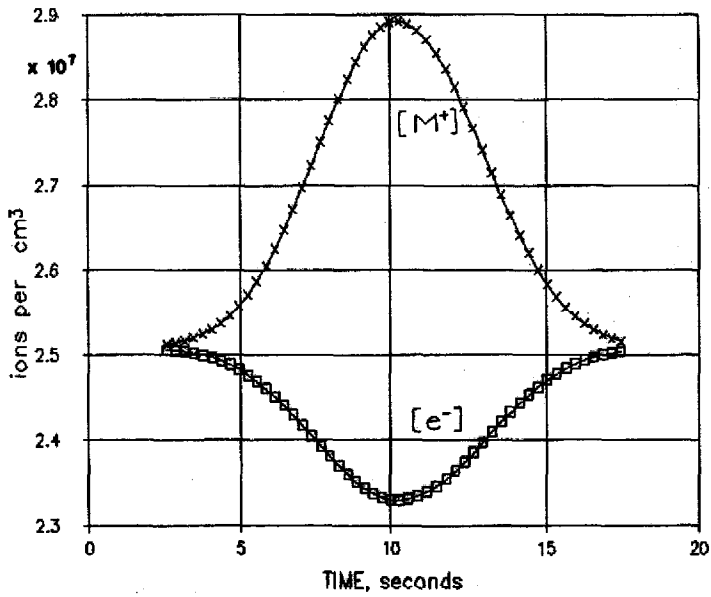

Fig. 23. Cation (×) and electron (□) concentrations during the passage of the Gaussian input peak shown in Fig. 21.

HCR value particular to that point. [Note that, as the peak rises and falls, the running HCR value will also change, but to have used the running as opposed to a particular HCR value would have meant distorting the peak shape. Since only a height normalization factor is used here (the latter process being equivalent to setting a suitable attenuation on the ECD electrometer) the output peak will maintain its characteristic appearance.]

Fig. 21 presents such a comparison of detector input and output. It shows an analyte peak of 0.125 pg SF_6 with a retention time of 10 and a σ of 2.5 s. Equation set 5–8 is used with the electron-capture constant of SF_6 from the literature $k_C = 3 \cdot 10^{-7}$ cm^3/s, with a ventilation rate of 2.86 s^{-1} for neutral SF_6, and with a pulse period of 1 ms. These simulated detector conditions are arguably quite "typical".

As expected from the ventilation rate and from the fact that the anion concentration, which controls response, needs a few tenths of a second to build up close to steady-state levels, the output peak is slightly off-set from the input peak, particularly on the down side. Note that this shift would have appeared even smaller if the HCR value of the output peak maximum (21.8 F/mol at 10.3 s) had been used for normalization instead of the HCR value at the true retention time (21.6 F/mol at 10.0 s). The important point is, however, that the peak shift is of the expected magnitude (a few tenth of a second) and that this small a distortion would hardly be noticed in typical gas chromatographic runs.

For general interest, the end-of-cycle analyte and ion concentrations are given in Figs. 22 and 23 for the passage of the same Gaussian peak. Not all analyte molecules have been converted to anions (a simulation result whose validity depends strongly on the chosen magnitude of the electron-capture and recombination constants). Cation and electron concentrations show the expect increase and decrease, respectively.

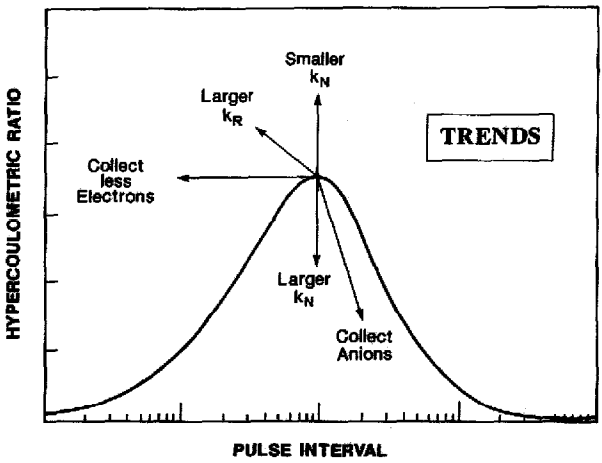

Fig. 24. Schematic of typical shifts in response profiles with changes in rate constants and collection efficiencies[28].

Simulation vs. experiment

By now the general behaviour of the simulated system is pretty well understood, at least as regards changes in the rate constants and the collection efficiencies for anions, electrons and cations. Fig. 24 summarizes these factors in an artist's rendition prepared for the 1987 CIC Conference[28]. Also understood are probable or typical effects resulting from ventilation and/or the use of Gaussian inputs. The diagnostic question therefore arises how well the *simulated* HCR *vs.* pulse period plots of this study correspond to the earlier *experimental* HCR profiles[7]. Aside from noting the immediately obvious similarity in appearance and pattern of the two, we shall compare them in greater detail in regard to their general shape, position on the time axis, and response amplitude.

The general *shape* of the typical response profile over a (logarithmic) range of pulse periods is, within the experimental variation, about the same for the two systems. In both cases do we see peaks of (very roughly) Gaussian shape, whose width at half height is (very approximately) one order of magnitude.

The *position* of the profiles on the pulse period axis is a more complicated matter. As mentioned before, the profiles of ref. 7 were measured with very short pulse widths (most frequently 0.5 μs) in an effort to establish that even a regime, whose pulse widths are negligible compared to its pulse-free intervals, can unambiguously produce hypercoulometry in a small-volume detector. That purpose was achieved[7] but, as a consequence, the reported HCR profiles had obviously been recorded at relatively low electron collection rates.

As Fig. 20 clearly demonstrated, a decrease in electron collection rates leads to a dramatic shift of the HCR maximum toward shorter pulse periods. Indeed, several of the experimental profiles peak at *ca.* 0.1 ms, while the simulations, which use a 100% electron collection rate, peak around 0.8 ms. According to Fig. 20, 0.1 ms corresponds to an electron collection rate of about 20%. That theoretical value is in actual agreement with some of the experimentally measured values. However, matters are not quite as simple as that.

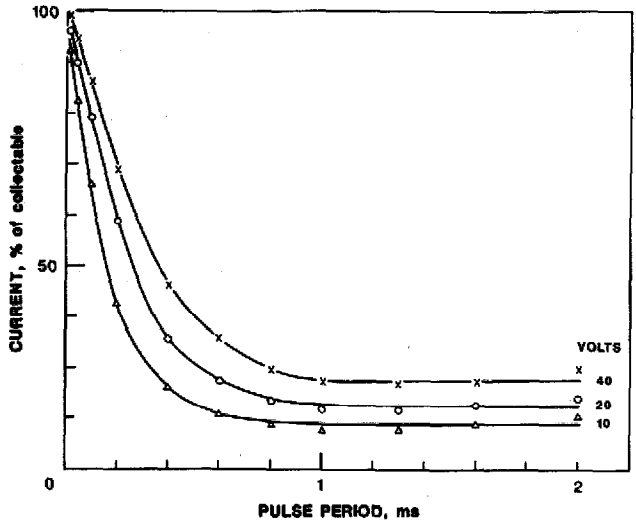

Fig. 25. Experimental electron collection efficiency in a Varian detector under a 80 ml/min nitrogen purge. Pulse width 0.5 μs. Pulse amplitude: × = 40 V; ○ = 20 V; △ = 10 V. The "collectable" current is measured by using 50 V–100 μs pulses, and corrected for electron generation during the pulse-on time.

Given a certain pulse width and amplitude, experimental percentages of electron collection obviously change with the pulse period. Even though the pulse may be extremely short, applying it very frequently will still collect most of the current. The "theoretically collectable" current also changes with the pulse period, owing to significant ion-pair recombination during long pulse-free intervals. Further, the experimental percent electron collection under clean conditions (where it can be measured, albeit with some difficulty) is not exactly the same as under doped conditions (where the response profiles are measured). The difference in system parameters under the two conditions is likely to derive, *inter alia*, from the different internal fields in the absence and presence of anions, from the different effects the

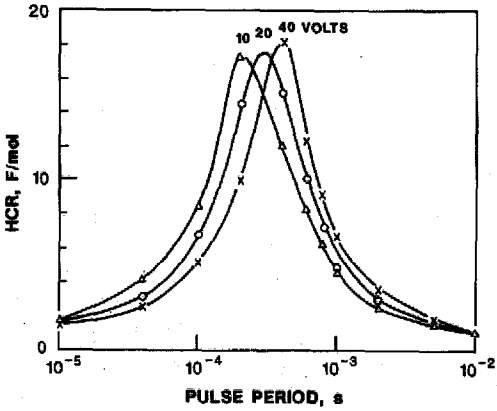

Fig. 26. Simulated response profiles, using separate, experimentally determined electron collection efficiencies (see Fig. 25) for each pulse period. DERKF only. From left to right: △ = 10 V; ○ = 20 V; × = 40 V.

withdrawal of electrons has on the chemically and kinetically dissimilar clean and doped systems, and from the different degrees of detector "contamination" with and without analyte load.

Yet, it was still considered worthwile to go back and obtain a rough *experimental* measure of the Varian detector electron collection efficiency under the pulse regimes of ref. 7, and then to introduce these values into the simulations —if only to show that such simulations are feasible. Fig. 25 shows the experimentally determined current as a percentage of the maximum collectable one. For the latter measurement, 50 V–100 μs pulses had to be used, with correction for the "pulse-on" time. The choice of conditions still represents a compromise, hence the percent current collection data of Fig. 25 should be considered upper values. These values can now be incorporated into the simulation, and response can thus be calculated with a *separate* electron collection efficiency for *each* pulse period. Fig. 26 shows the result of this simulation.

The agreement between simulation and experiment is good but not ideal; this is not totally unexpected in light of the differences in shape that the experimental profiles show even among themselves. The simulated profiles do exhibit the expected shift to lower pulse periods with decreased voltage (electron collection), however, the position of the maxima on the time scale, while well within the correct order of magnitude, still differs between the simulated and the experimental SF_6 systems. Also, the simulated profiles bunch closer together than the experimental ones do. Whether this represents, as discussed above, merely an effect of different collection efficiencies in clean *vs.* doped systems, or whether it is mostly due to experimental variability, or whether (heaven forbid) the model still continues to neglect some crucial, real-life aspect of the ECD, remains unclear at present.

Of the processes that are sufficiently understood, there are at least two that could shift experimental response profiles to shorter pulse periods. These processes are an increase in the apparent recombination rate constant during the passage of a peak (compare Fig. 14), and a delay in the collection of cations (a temporary electrical imbalance following each pulse, compare Fig. 18). An increased apparent recombination rate in the detector during the passage of a peak is actually quite likely to occur, if only because the positive charge should easily transfer from (mainly) N_4^+ to some lower-energy species. The effect is akin to the experimental fact that, the dirtier a detector and its carrier gas, the higher will the experimentally determined recombination rate constant. Given the likelihood of such effects, the relatively minor difference in position of the experimental and simulated profiles appears quite acceptable.

That leaves the *amplitudes* of the simulated response profiles to be considered, which are considerably higher than the experimental ones. This would appear to indicate a problem in the simulations. However, it is actually very easy to simulate a well-fitting profile by a variety of means. For instance, using the electron-capture constant from the literature and introducing a fast carrier flow reduces the simulated response already by about one third (compare Fig. 10 and 11). To bring the HCR value then down from *ca.* 12 F/mol to the experimental SF_6 value of *ca.* 4 F/mol would require only an anion collection rate of about 5% (see Fig. 17), or a shift in the recombination or neutralization constant by a factor of less than 10 (see Figs. 13 and 14). In fact, just using the "best" literature values for the two constants (rather than our own measurements) would make the simulation come very close to the experiment.

A reduction in response could also be achieved by assuming that the literature value of the electron-capture constant for SF_6 was higher than the corresponding apparent constant in the detector, or that the steady state had not been reached for some or all of the measurement time, owing to the fast flow. (To turn the problem around, one can of course also assume —and with higher credibility— that the real-life detector and its carrier gas had not been as absolutely clean as the mathematical simulation but, had they been, higher HCR values would have resulted from the experiment.)

Since several kinetic parameters, or a combination of these, or experimental manipulation, all could be used to equalize the two systems, and since there is no reasonable way for us to decide which of the several possible avenues would be the correct one(s) to take, we refrain from taking any. We conclude however that, on the face of it, the experimental and the simulated profiles appear very similar and, given some slight changes in simulation parameters, could easily be made to coincide within experimental error limits.

The current study has thus clearly demonstrated the probability of a kinetically driven process of gas-phase response amplification, resulting in observable hypercoulometry "of the second kind". We suggest that such a process is responsible, at least in part, whenever hypercoulometric behaviour is shown by (particularly) a small-volume detector, and that it contributes to response in large-volume detectors as well. We further suggest that such kinetics are also involved in conventional (*hypo*coulometric) response.

Conventional ("hypocoulometric") response

This study appeared to deal almost exclusively with *hyper*coulometric response, *i.e.* with the experimentally observable condition that HCR > 1 F/mol. However, the "explanation" of this effect, as given here, does not rely on any circumstances unique to hypercoulometry. Rather, the equations and conditions used are general for *any* ECD response. And, while examples of hypercoulometry are plentiful, the overwhelming majority of peaks seen by the detector is definitely hypocoulometric (HCR < 1 F/mol). In part this is due to the less than perfect performance of real-life detectors (both their construction and contamination may play a role here) and in part this simply reflects the fact that the electron-capture constants of many typical ECD analytes may not be large enough to result in observable hypercoulometry.

However, the processes that determine response, *i.e.* the non-collection of anions that results in accelerated electron–cation recombination, as well as the removal of electrons by the capture reaction itself, are the same whether a particular analyte produces hyper- or hypocoulometric peaks. Given a specific detector running under specific conditions, the percentage of response that is caused by the accelerated electron recombination (as well as that caused by the initial electron capture) should be roughly the same for any peak. Response, whatever the detector and its conditions, represents the combined effects of more than one process. Obviously, the more sensitive type of detectors will generally be the ones that make it more difficult for the anions to be collected.

Those are the detectors in which considerably more electrons are removed from the baseline current than anions are formed from the analyte, *i.e.* those that promote gas-phase amplification. However, even KAR, as defined by eqns. 14 or 15, may often fall below unity. The reason is merely one of definition: KAR, in order to be compared

with the directly measurable HCR, was defined by using the (experimentally known) analyte input rate (as opposed to the experimentally unknown anion generation rate). Simulation-wise this made no difference when equation set 9–12 was used, and little difference when a large value of k_C and a small value of S_A were employed with set 5–8, *i.e.* when the analyte was a strong capturer present at a low concentration. With weaker capturers and/or larger concentrations, however, the fact that the rate at which electrons are removed from the background current (the "response") greatly exceeds the rate of capture events, may not be so immediately obvious. Yet, one may formally argue that the true kinetic *amplification* takes place only *after* anions are formed. If so, one can define a different, "true" kinetic amplification ratio, KAR′

$$\mathrm{KAR}' = \frac{\frac{\mathrm{d}[e^-]_0}{\mathrm{d}t} - \frac{\mathrm{d}[e^-]}{\mathrm{d}t}}{S_{A^-}} \ \mathrm{F/mol} \tag{24}$$

wherein S_{A^-}, the anion generation rate, equals $k_C[A][e^-]$. The resulting KAR′ values would, of course, be equal to the KAR value for an infinitely fast electron capturer (the anions of which would have similar speed and reactivity). A comparable change, substituting S_A by the average rate of anion formation per second in eqn. 16, would likewise produce a "true" hypercoulometric ratio, HCR′, in faradays of peak area per moles of *anions* generated. Again, such an HCR′ value should be similar to the HCR value for a perfect capturer, and should remain fairly constant for electron capturers of all degrees of strength under a given set of circumstances. The only apparent differences should, again, relate to the different mobilities of anions (if some are indeed collected) and their different neutralization constants.

In this context it would be interesting to determine *experimentally* the fraction of analyte that is actually converted to anions. Some estimates can be obtained by following the disappearance of (strongly capturing) analyte molecules in the detector, by attaching the latter to a second column feeding yet another detector. While interesting in their own right, the usefulness of such measurements[29,30] for the purpose at hand would obviously be in doubt if certain secondary processes (anion → analyte recycling, formation of electron-capturing products, etc.) could not be excluded.

To return to the consideration of ECD response, the conclusion now appears warranted that *some* gas-phase amplification must occur in *any* detector, whether capable of producing hypercoulometric response or not.

Note added in revision

One of the reviewers of this manuscript suggested that the developed simulation model would fail to produce linear response for weak capturers (*i.e.* that it would be in conflict with experimental evidence) and requested that calibration curves be simulated for weak capturers in order to confirm or deny the validity of the model. Even though we are not primarily interested in weak capturers and, furthermore, view as doubtful the diagnostic quality ascribed to a linear calibration, we are pleased to comply with his request.

In light of the earlier discussion, a weak capturer, should in first approximation behave just like (much smaller amounts of) a strong capturer. The only real criterion for response is how many anions are created (and how the detector translates this

number into an externally observable signal). Thus one would predict that the linearity of response, measured by the effect the analyte has on the system, *i.e.* by the percent reduction in available electron current, should not be much different among all kinds of capturers, weak or strong. Any differences in linear range, at least as perceived at present, could only relate (a) to the decrease in anion generation rate (eqn. 7) caused by depletion of a very strong capturer (as opposed to a weak capturer, the concentration of which is not significantly reduced by the capture reaction) and/or (b) to the differences in time spent in approaching or attaining steady state. These effects should generally be of minor importance, though, when compared with the fact that each linear range from a series of calibration curves must be limited at its upper end by the same diminishing supply of electrons.

For simulating the calibration curves of weak, and comparing them to those of strong capturers, a set of suitable conditions has to be chosen. These conditions should be typical of the electron-capture detector, allow reference to other data of this manuscript, and facilitate comparability. Consequently we selected a 1-ms pulsing regime with 100% electron collection, zero anion collection, and fast analyte ventilation ($F/V = 2.86\ s^{-1}$). Analytes were introduced on a constant-rate basis and all calculations were carried on for a simulation time of 1 s (more than enough in most cases to reach steady state). Response was computed as a percentage of baseline current, and the final levels for HCR and all particle concentrations were also recorded. The rate constants were the same as used in earlier simulations, except that the fictitious analytes were given capture constants of (a) infinity (instantaneous and complete conversion into anions), (b) $1 \cdot 10^{-6}$ (as high as one is likely to encounter), (c)

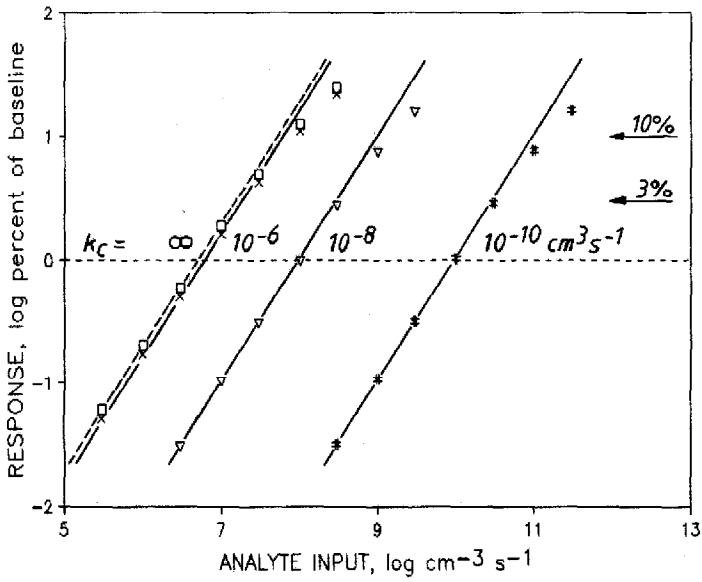

Fig. 27. Simulated calibration curves of strong and weak capturers. Time unit 100 μs, pulse period 1 ms, simulated time 1 s. Complete electron collection, no anion collection. Analyte ventilation = 2.86 s^{-1}, $k_R = 2.9 \cdot 10^{-5}$, $k_N = 3.8 \cdot 10^{-7}$ cm^3/s (for all analytes). Capture constants (from left to right): □ = $1 \cdot 10^{-4}$ (practically equal to infinity); × = $1 \cdot 10^{-6}$; ▽ = $1 \cdot 10^{-8}$; # $1 \cdot 10^{-10}$ cm^3/s. SC3.

$1 \cdot 10^{-8}$, and (d) $1 \cdot 10^{-10}$ cm^3/s. Still smaller values of k_C were also tested, but they added nothing to the picture.

Fig. 27 summarizes the results of the various simulations. The straight lines are drawn precisely at unity slope. The linear range (definition: within 0 to -10% of response) ends for all analytes at 3 to 4% of baseline current. The dashed line marks the limiting case $S_A = S_{A^-}$.

Three aspects become immediately obvious from Fig. 27. First, there is no appreciable difference between strong and weak capturers as far as the linearity of their calibration curves is concerned. The upper end is essentially determined by the availability of electrons, hence equal for all analytes. Second, the horizontal distance between $k_C = 10^{-8}$ and 10^{-10} is two units, *i.e.* two orders of magnitude in response (note: $k_C = 10^{-12}$ would occur a further two units to the right, etc.). That information can, of course, be gleaned directly from the rate law for anion generation (provided a *weak* capturer is the source of anions and provided it is truly the latter that control response). Third, curves for compounds with large capture constants (strong capturers) bunch up close to the dashed limit. That simply means that no analyte can do more than convert completely to anions. However, it should be noted in this context that the present simulation neglects to consider the potential occurrence of anion-neutral recycling, electron-capturing products, limiting collision rates, and other processes that could increase or decrease the number of anions obtainable.

Thus, in the linear region the response of weak capturers is determined by their capture constant (and, of course, the magnitude of response amplification as dependent on the particular detector system and the mobility and reactivity of the respective anions) while the response of strong capturers is essentially determined by

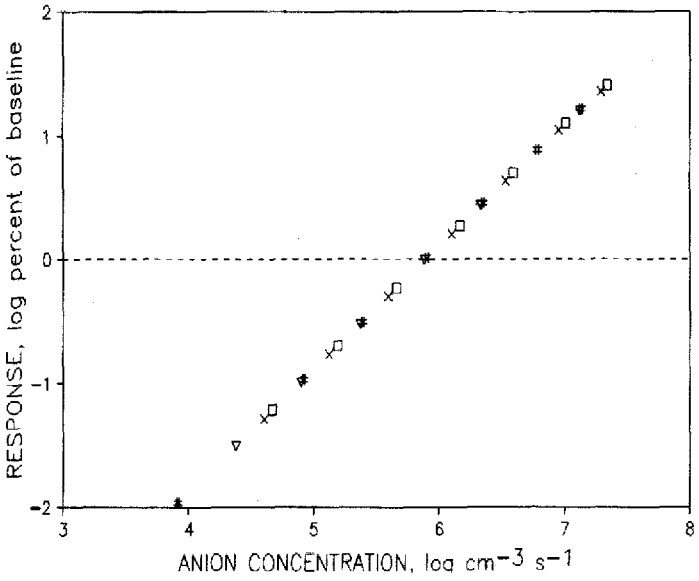

Fig. 28. Response (as percent reduction of baseline current) *versus* end-of-cycle anion concentrations. Symbols and simulations as in Fig. 27. Note that the *same* value of k_N (equal to the experimental value for SF_6) has been used for *all* analytes.

the absolute number of their molecules. The transition region between the perfectly strong and the manifestly weak capturer involves the contributions of *two* limiting factors, so the upper end of the linear range may show that. However, the effect, if any, should be slight.

While implicit in the simulation scenario, the importance that anions have for ECD response has not yet been graphically demonstrated in this manuscript. The calibration curves of strong and weak capturers afford a good opportunity to remedy this omission: the anion concentrations from a range of input levels of the four different capturers from Fig. 27 are easily available and can be directly compared with the magnitude of the corresponding responses. This is shown in Fig. 28, wherein all data fall onto *one* straight line of unity slope. All capturers, including one of infinite strength, behave alike in this type of plot. This confirms, as speculated earlier, that the *anion*-based, "true" amplification parameters KAR′ (eqn. 24) and HCR′ of any analyte, regardless of its capturing ability, would be equal to those of a perfect capturer.

There is only one minor hitch in this scenario. The simulation demanded input values for the neutralization constants of every type of anion —but only one such value, namely that of the anion(s) from SF_6, had ever been experimentally determined in the model detector (in fact, the constant of a weak capturer could not have been so determined since the measurement was based on the exhaustive conversion of analyte molecules to anions[11]). Having no other available, we used the SF_6 constant for *all* the fictitious analytes. This ensured comparability but violated the individuality of real analytes: the neutralization constants of various anions do differ, and so do their mobilities. In practical terms, however, such differences fall more or less within one order of magnitude and, had different constants been incorporated into the different simulations, the single line of Fig. 27 would simply have been replaced by a close bundle of lines, one for each neutralization constant: the linear range of these calibration curves would still have remained the same.

ACKNOWLEDGEMENTS

Part of this study was supported by NSERC operating grant A-9604. The many interesting and helpful discussions with A. McMahon are greatly appreciated.

REFERENCES

1 J. E. Lovelock, R. J. Maggs and E. R. Adlard, *Anal. Chem.*, 43 (1971) 1962.
2 D. Lillian and H B. Singh, *Anal. Chem.*, 46 (1974) 1060.
3 J. E. Lovelock, *J. Chromatogr.*, 99 (1974) 3.
4 E. P. Grimsrud and S. H. Kim, *Anal. Chem.*, 51 (1979) 537.
5 E. P. Grimsrud and S. W. Warden, *Anal. Chem.*, 52 (1980) 1842.
6 S. Kapila and W. A. Aue, *J. Chromatogr.*, 118 (1976) 233.
7 K. W. M. Siu, G. J. Gardner and S. S. Berman, *J. Chromatogr.*, 330 (1985) 87.
8 W. A. Aue and S. Kapila, *J. Chromatogr.*, 188 (1980) 1.
9 A. McMahon, *Doctoral Thesis*, Dalhousie University, Halifax, 1987.
10 A. W. McMahon and W. A. Aue, *Mikrochim. Acta*, III (1988) 11.
11 K. W. M. Siu, S. S. Berman and W. A. Aue, *J. Chromatogr.*, 408 (1987) 53.
12 K. W. M. Siu and W. A. Aue, *Can. J. Chem.*, 65 (1987) 1012.
13 K. W. M. Siu and W. A. Aue, *J. Chromatogr.*, 392 (1987) 143.
14 E. D. Pellizzari, *J. Chromatogr.*, 98 (1974) 323.

15 A. Zlatkis and C. F. Poole (Editors), *Electron Capture —Theory and Practice in Chromatography (Journal of Chromatography Library*, Vol. 20), Elsevier, Amsterdam, 1981.
16 L. G. Christophorou, *J. Phys. D.*, 14 (1981) 1889.
17 R. Simon and G. Wells, *J. Chromatogr.*, 302 (1984) 221.
18 W. A. Aue, K. W. M. Siu and S. S. Berman, *J. Chromatogr.*, 395 (1987) 335.
19 J. L. Pack and A. V. Phelps, *Phys. Rev.*, 121 (1961) 798.
20 F. W. Karasek, *Anal. Chem.*, 46 (1974) 710A.
21 M. W. Siegel and M. C. McKeown, *J. Chromatogr.*, 122 (1976) 397.
22 P. L. Gobby, E. P. Grimsrud and S. W. Warden, *Anal. Chem.*, 52 (1980) 473.
23 M. W. Siegel, *11th International Symposium on Chromatography, Birmingham, July 1976*, review lecture.
24 E. P. Grimsrud, S. H. Kim and P. L. Gobby, *Anal. Chem.*, 51 (1979) 223.
25 W. A. Aue and K. W. M. Siu, *J. Chromatogr.*, 239 (1982) 127.
26 N. G. Adams, D. Smith and C. R. Herd, *Int. J. Mass Spectrom. Ion Proc.*, 84 (1988) 243.
27 S. Kapila and W. A. Aue, *J. Chromatogr.*, 148 (1978) 351.
28 W. A. Aue, A. McMahon, K. W. M. Siu and S. S. Berman: *Gas-Phase Amplification Mechanisms in the Electron Capture Detector, 70th Canadian Chemical Conference, Chemical Institute of Canada, Quebec City, June 1987.*
29 S. Kapila and W. A. Aue, *J. Chromatogr.*, 108 (1975) 13.
30 S. Kapila, C. R. Vogt and W. A. Aue, *J. Chromatogr.*, 196 (1980) 397.